MAJOR REPORT • **OPEN ACCESS**

Physics with high-luminosity proton-nucleus collisions at the LHC*

OPEN ACCESS
IOP Publishing
Journal of Physics G: Nuclear and Particle Physics
J. Phys. G: Nucl. Part. Phys. **52** (2025) 090501 (28pp)
https://doi.org/10.1088/1361-6471/adeda5

Major Report

Physics with high-luminosity proton-nucleus collisions at the LHC*

D d'Enterria[1,†], C A Flett[2,†], I Grabowska-Bold[3,†], C Hadjidakis[2,†], P Kotko[3,†], A Kusina[4,†], J P Lansberg[2,†], R McNulty[5,†,], M Rinaldi[6,†], L Bonechi[7,‡], R Bruce[8,‡], C Da Silva[9,‡], E G Ferreiro[10,‡], S Fichet[11,‡], L Harland-Lang[12,‡], G Innocenti[13,‡], F Jonas[14,‡], J M Jowett[1,15,‡], R Longo[16,‡], K Lynch[2,5,‡], C McGinn[13,‡], T Pierog[17,‡], M Pitt[1,‡], S Redaelli[8,‡], B Schenke[18,‡], I Schienbein[19,‡], M Stefaniak[20,‡], M Strikman[21,‡], L Szymanowski[22,‡], D Tapia Takaki[23,‡], C Van Hulse[24,‡] and S Wallon[2,‡]**

[1] CERN, EP Department, 1211 Geneva, Switzerland
[2] Université Paris-Saclay, CNRS, IJCLab, 91405 Orsay, France
[3] AGH University of Krakow, Faculty of Physics and Applied Computer Science, Krakow, Poland
[4] Institute of Nuclear Physics, Polish Academy of Sciences, PL-31342 Krakow, Poland
[5] School of Physics, University College Dublin, Dublin 4, Ireland
[6] Dipartimento di Fisica, Universitá degli studi di Perugia, and INFN Sezione di Perugia. Via A. Pascoli, Perugia, 06123, Italy
[7] INFN, Sezione di Firenze, Via B. Rossi 1, Sesto Fiorentino 50019, Italy
[8] CERN, BE Department, 1211 Geneva, Switzerland
[9] Los Alamos National Laboratory (LANL), Los Alamos, NM, United States of America
[10] Instituto Galego de Física de Altas Enerxías, Univ. Santiago de Compostela, E-15782, Galicia, Spain
[11] CCNH, Universidade Federal do ABC, Santo André, 09210-580 SP, Brazil
[12] Department of Physics and Astronomy, University College London, London, WC1E 6BT, United Kingdom
[13] Massachusetts Institute of Technology, 371 Richmond Blvd, Ronkonkoma, NY 11779, United States of America
[14] Lawrence Berkeley National Laboratory, Berkeley, CA, United States of America
[15] GSI Helmholtzzentrum für Schwerionenforschung GmbH, Darmstadt, Germany
[16] Department of Physics, University of Illinois at Urbana-Champaign, Urbana IL, United States of America
[17] Karlsruhe Institute of Technology (KIT), Institute for Astroparticle Physics, D-76021 Karlsruhe, Germany

* This is a slightly expanded version of a contribution submitted for the 2025 European Strategy for Particle Physics. Its original version can be found at https://indico.cern.ch/e/pA4LHC along with the list of the 150+ people who endorsed it.

[18] Physics Department, Brookhaven National Laboratory, Upton, NY 11973, United States of America
[19] Lab. Physique Subatomique et Cosmologie, Univ. Grenoble-Alpes, CNRS/IN2P3, 53 Av. des Martyrs, 38026 Grenoble, France
[20] The Ohio State University, Department of Physics, 191 Woodruff Avenue, Columbus, OH 43210, United States of America
[21] Penn State University, University Park, PA 16802, PA, United States of America
[22] National Centre for Nuclear Research (NCBJ), Pasteura 7, 02-093 Warsaw, Poland
[23] Department of Physics and Astronomy, The University of Kansas, Lawrence, KS, 66045, United States of America
[24] Universidad de Alcalá, Alcalá de Henares, Spain

E-mail: ronan.mcnulty@ucd.ie

Received 21 April 2025
Accepted for publication 9 July 2025
Published 22 September 2025

Abstract

The physics case for the operation of high-luminosity proton-nucleus (pA) collisions at the CERN LHC is reviewed. The collection of $\mathcal{O}(1\text{–}10\,\mathrm{pb}^{-1})$ of proton-lead (pPb) collisions at the LHC will provide unique physics opportunities in a broad range of topics including proton and nuclear parton distribution functions (PDFs and nPDFs), generalised parton distributions (GPDs), transverse momentum dependent PDFs (TMDs), low-x quantum chromodynamics and parton saturation, hadron spectroscopy, baseline studies for quark-gluon plasma and parton collectivity, double and triple parton scatterings, photon–photon collisions, and physics beyond the Standard Model; which are not otherwise as clearly accessible by exploiting data from any other colliding system at the LHC. This report summarises the accelerator aspects of high-luminosity pA operation at the LHC, as well as each of the physics topics outlined above, including the relevant experimental measurements that motivate much larger pA datasets than collected to date.

Keywords: proton-nucleus collisions, LHC, proton/nuclear distribution functions, QCD, spectroscopy, quark-gluon plasma

1. Introduction

This document reports the physics case for an ambitious proton-nucleus (pA) collision program at the CERN LHC in the context of the forthcoming update of the European strategy for

† Editor.
‡ Contributor.
** Author to whom any correspondence should be addressed.

particle physics. Following the accelerator and physics studies outlined in [1, 2], and a short pilot run to demonstrate feasibility in 2012, the LHC operated *p*Pb collisions at nucleon–nucleon (*NN*) center-of-mass (CM) energies of $\sqrt{s_{NN}} = 5.02,\ 8.16$ TeV in 2013 and 2016, respectively, but no run has been performed since then, and none is currently planned for the near future. The past *p*Pb runs have brought essential contributions to particle, heavy-ion, and cosmic-ray physics, leading to, among others, significantly improved nuclear parton distributions functions (nPDFs) [3], and the discovery of new phenomena, such as the onset of parton collectivity [4]. As discussed hereafter, high-luminosity *pA* collisions in Run 3 and 4 at $\sqrt{s_{NN}} = 8.54$ TeV, involving both heavy and light nuclei, are essential to fully exploit a rich experimental program for the study of quantum chromodynamics (QCD) in the perturbative, nonperturbative, and high-density regimes. They provide, in particular, a unique and complementary environment for uncovering the tomography of the proton and nuclei, and their partonic properties.

Compared to *pp* collisions, *pA* interactions allow the exploration of nuclear modifications to PDFs and cold nuclear matter effects, which are essential for understanding the initial-state conditions of heavy-ion collisions. Additionally, *pA* collisions probe small-x physics more effectively than *pp*, providing insight into gluon saturation and the onset of nonlinear QCD effects, which are enhanced due to the intrinsically larger number of initial partons [5].

Compared to *AA* collisions, *pA* collisions offer higher nucleon–nucleon CM energies, higher luminosity, and a cleaner environment, free from the final-state complexities of a fully-developed quark-gluon plasma (QGP), making them an essential benchmark for interpreting heavy-ion data, while studying the onset of collectivity in small systems. Photoproduction in *pA* collisions, which capitalizes on the LHC as a photon-collider, complements the ultra-peripheral-collisions (UPCs) program in *AA* collisions [6], and has many benefits through being able to distinguish the more energetic photon emitter.

Investigations of quarkonium production [7], exotic hadrons, scenarios beyond the Standard Model (BSM), and hadronisation mechanisms, can all be performed in detail in an environment that bridges the gap between *pp* and *AA* systems, and improves our understanding of ultrahigh-energy cosmic-ray interactions [8], underscoring the importance of *pA* data in advancing our knowledge of high-energy nuclear, particle, and astroparticle physics. The data taken in *pA* collisions at Run 1 and 2 of the LHC program has had a major impact for all these fields, extrapolating precise knowledge of proton collisions to multi-nucleon systems. The novel use of these collisions has brought significant advances to our understanding of both the proton and the nucleus. The Run 3 plan discussions have focused so far on *pp* and *AA* collisions: the absence of *pA* collisions to date is notable and appears as a missed opportunity. This document presents a summary of the accelerator and physics case aspects needed to revert this trend.

2. Accelerator and detector considerations

The LHC has been designed to collide protons and nuclei at a beam energy of $7Z$ TeV (where Z is the ion electric charge) [9] and up to $6.8Z$ TeV has been achieved to date. The LHC typically operates about one month per year with heavy-ion beams, mainly fully stripped Pb nuclei. Initially, the heavy-ion program consisted only of PbPb collisions, and it was then extended with a new mode of operation with proton-nucleus collisions [1, 2, 10–13]. Following initial pilot tests, two 1-month physics runs with *p*Pb collisions were carried out in 2013 and 2016, with integrated luminosities of $\mathcal{L}_{\rm int} \approx 220\,{\rm nb}^{-1}$ collected in ATLAS and CMS, $75\,{\rm nb}^{-1}$ in ALICE, and $36\,{\rm nb}^{-1}$ in LHCb, combining the data in Run 1 (2010–2013)

Table 1. Delivered integrated luminosities in *p*Pb collisions in Run 1 and Run 2, $\mathcal{L}_{\rm int}$ targets in *p*Pb collisions in Run 3 and 4, and number of runs needed to achieve these $\mathcal{L}_{\rm int}$ with the presently predicted performance.

	ALICE	ATLAS/CMS	LHCb
Total $\mathcal{L}_{\rm int}$ delivered in Run 1 and Run 2 ($\rm nb^{-1}$)	75	220	36
Target $\mathcal{L}_{\rm int}$ for Run 3 and Run 4 ($\rm pb^{-1}$)	0.6	1.2	0.6
Projected $\mathcal{L}_{\rm int}$ per 1-month run ($\rm pb^{-1}$) [21]	0.33	0.47	0.15
Number of runs needed to reach targets	1.8	2.5	4

and Run 2 (2015–2018). The heavy-ion operation in the ongoing Run 3 (scheduled from 2022 to mid 2026) has consisted of two PbPb runs so far. In the future, collisions with Pb ions are scheduled to continue with 1-month heavy-ion operation in most operational years until the end of Run 4 (scheduled for 2030–2033). Operation with *p*Pb is included in this plan, but the detailed PbPb and *p*Pb time allocations have not yet been decided. The goals for future *p*Pb operation, combining Run 3 and Run 4, are $\mathcal{L}_{\rm int} = 1.2\,\rm pb^{-1}$ at ATLAS and CMS, and $0.6\,\rm pb^{-1}$ at ALICE and LHCb [14]. The next opportunity for *p*Pb operation might come already in 2026, however, the decision has not yet been taken. In addition to high-intensity *p*Pb operation, a short low-intensity *p*O run is planned for mid-2025 [15].

The assumed LHC scenario for future *p*Pb operation considers the same machine cycle as for PbPb [16], relying on crystal collimation [17], and round optics with $\beta^* = 0.5\,\rm m$ at ALICE, ATLAS, and CMS. However, a more complicated setup of the radiofrequency (RF) system is needed. Because of the difference in charge-to-mass ratio between protons and Pb, the two species have different revolution frequencies at equal momentum per charge. Therefore, both beams have to be brought off-momentum in different directions by the RF cavities to equalize their frequencies, such that the longitudinal locations of the collision points are stationary. This momentum offset is introduced only at top energy due to aperture constraints. An additional challenge is the beam-beam effect between the asymmetric beams and the moving long-range beam-beam encounters [13, 18]. We assume the same structure of the Pb beam as in PbPb operation, with 50 ns bunch spacing by interleaving different bunch trains longitudinally in the SPS ('slip-stacking'), and an opposing 50 ns proton beam with low intensity. The proton beam is produced in a different way by the injectors, and a perfect overlap between the two beams cannot be obtained, resulting in slightly fewer colliding bunches per experiment. It is also assumed that only ALICE needs luminosity levelling at $5 \times 10^{29}\,\rm cm^{-2}\,s^{-1}$ in order to limit the event rate to about 1 MHz.

The projected future luminosity performance in single *p*Pb fills have been simulated with the CTE code [19] extrapolated over a full 1-month run [20]. Recent calculations with updated filling schemes give projected $\mathcal{L}_{\rm int} \approx 0.33\,\rm pb^{-1}$ at ALICE, $0.47\,\rm pb^{-1}$ at ATLAS/CMS, $0.15\,\rm pb^{-1}$ at LHCb, for a 1-month run (24 d of physics) at $\sqrt{s_{NN}} = 8.54$ TeV (6.8Z TeV beam energy). These numbers carry large uncertainties and depend highly on machine availability and achieved beam parameters. If *p*Pb collisions are performed at the lower PbPb beam energy, to be used as reference data for the latter and profiting from the same *pp* reference data set, the luminosity would be reduced. Table 1 summarizes the delivered $\mathcal{L}_{\rm int}$, the targets for future runs, the projected $\mathcal{L}_{\rm int}$ per run, and the number of runs needed to reach the targets. We note that one day of high-luminosity *p*Pb running corresponds to 10%–20% of the total $\mathcal{L}_{\rm int}$ gathered thus far. Given that up to four 1-month runs are needed to reach the

target $\mathcal{L}_{\rm int}$, and there will likely be at most two *p*Pb runs until the end of Run 4, several ways of improving the performance are being explored.

Increasing the Pb intensity, which might be within reach based on the injector performance in 2024 and on the upgrades deployed at the LHC [22], is a good way forward, but likely not enough to reach the targets at all IPs in two runs. Decreasing the proton-beam bunch spacing to 25 ns, as used in standard *pp* operation, allows for more collisions at LHCb without penalizing other experiments. The peak luminosity can be further increased with higher proton bunch intensity, which would benefit all experiments except ALICE, assumed to be levelling. Further improvements might come from reduced β^* and crossing angles. However, studies are needed to investigate the feasibility of all these measures, e.g. in view of the much stronger beam-beam effects, as well as beam instrumentation in case of very asymmetric beams. It therefore remains as future work to investigate realistic scenarios where all experiments meet their $\mathcal{L}_{\rm int}$ targets.

In Run 4, the *p*Pb program will benefit from improved experimental setups, including enhanced forward detection capabilities (e.g. extended ATLAS and CMS trackers over $|\eta| < 4$ [23, 24] and ALICE FoCal with $3.2 < \eta < 5.8$ [25]), and forward proton detectors (e.g. CMS PPS [26]). Beyond Run 4, ion operation at the LHC is forecast to continue, including the planned ALICE 3 detector [27] for Run 5 and beyond. The main goal for this period will be to produce significantly higher nucleon–nucleon luminosities, and other nuclei than Pb are being investigated. Studies of achievable intensities for a range of ion species are ongoing in the CERN injector complex. A detailed program for this period has not been elaborated yet, and *pA* collisions might be included. Initial studies of the foreseen performance have been presented in [13, 28], although the achievable ion bunch intensities will need to be revised in the future. Furthermore, as there are no technical limitations to colliding protons with other nuclei than Pb, short low-intensity runs in such configurations may be envisaged, similarly to the planned oxygen run in 2025, although they are not yet part of the official LHC plan.

3. The physics case

The physics case for high-luminosity (HL) proton-nucleus collisions at the LHC is summarized in nine subsections below, each covering the following research topics: (i) constraints on nuclear parton distribution functions, (ii) constraints on proton generalized parton distributions (GPDs) and PDFs, (iii) small-x QCD and gluon saturation physics, (iv) benchmark for QGP physics and onset of collectivity, (v) double and triple parton scatterings, (vi) spectroscopy of bound states, (vii) photon–photon collisions, (viii) beyond the Standard Model physics, and (ix) connections to ultra high-energy cosmic rays.

3.1. Constraints on nuclear parton distribution functions (nPDFs and nTMDs)

Nuclear parton distribution functions (nPDFs) describe nuclei in terms of quarks and gluons, carrying a given longitudinal momentum fraction x at a factorization scale μ, and are essential universal ingredients in the description of all high-energy nuclear processes based on perturbative QCD (pQCD). When the parton density description is extended to explicitly incorporate the transverse momentum ($k_{\rm T}$) of the incoming partons, they are called nuclear Transverse Momentum Dependent PDFs (nTMDs). Before LHC *p*Pb data were available, knowledge of nPDFs was relatively scarce and mostly limited to lepton DIS on fixed-target nuclei. This provided information in the rather narrow region $0.01 < x < 0.2$ for up and down valence quarks alone, whereas the gluon and strange nPDFs were essentially unknown and

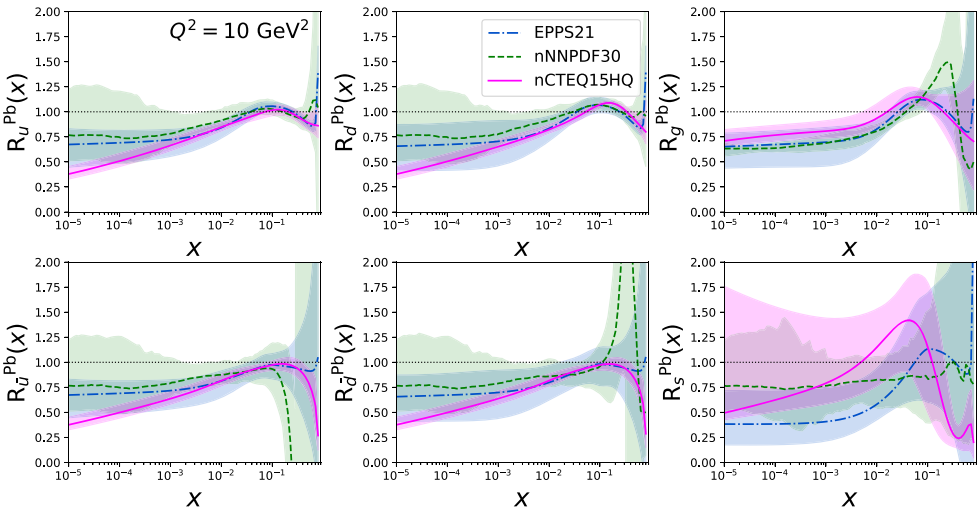

Figure 1. Comparison of nPDF nuclear modification factors for ^{208}Pb (i.e. the parton densities of lead divided by the averaged PDFs of 82 free protons and 126 free neutrons) for different parton species from various global analyses. Uncertainty bands correspond to 90% CL.

arbitrarily fixed by different nPDF parametrisations [29–33]. After limited *p*Pb LHC running, the situation today is very different as summarized in figure 1. Most of the parton densities are known with a precision better than 20% in the region $10^{-5} < x < 0.1$. This is a major improvement compared to pre-LHC times, and it needs to be highlighted that this was achieved solely thanks to *p*Pb data. Nevertheless, the current nPDF uncertainties are still insufficient for performing precise theoretical calculations of any process involving nuclei, including heavy ions at colliders and cosmic-ray interactions. Disentangling cold nuclear-matter effects in the initial and final states, separating beyond-DGLAP parton evolution (saturation and BFKL) from other nuclear effects, or studying the QGP in PbPb collisions all depend on the baseline description obtained with nPDFs.

A critical component for studying QCD with heavy ions is better information on the gluon nPDF in both the high and very low x regions. Some access to high-x gluons is provided by the fixed-target SMOG2 program at the LHC [34, 35], while moderate-x values can be probed at the EIC [36]. However, low-x gluons are uniquely accessible in *p*Pb collisions. The *pA* running to date has given some constraints on the low-x ($x \sim 10^{-5}$) gluon distribution [37–41]. However, this information comes solely from the heavy-flavor measurements (D, B, and quarkonium production) which are also sensitive to final-state nuclear effects [42]. Similar problems hold when searching for saturation or studying low-x evolution, see section 3.3. To disentangle different effects, more data in the low-x region are required, where a promising candidate is coherent J/ψ photoproduction on the nucleus in *pA* UPCs [6].

Although the photon is usually emitted from the nucleus, when it comes from the proton, its (much) higher longitudinal energy leads to differently boosted final states through which the events can be distinguished. However, the cross section is low, and sufficient statistics for PDF constraints require high luminosity. The $x \lesssim 10^{-3}$ region can also be studied in *pA* collisions through measurements of Drell–Yan (DY), isolated photons, W, and Z boson production at forward rapidities using LHCb and ALICE detectors [3]. For mid- and high-x gluon nPDFs, the cleanest probe is top-quark production, where sufficient statistics to obtain

precise differential distributions [43, 44] require high luminosity: the current data is only sufficient to extract the total $t\bar{t}$ cross section [45, 46]. Another option for constraining the mid-x gluon is inclusive jet or dijet data, as well as γ + jet and Z + jet measurements [47]. Furthermore, the measurement of $\gamma+$ heavy-quark allows probing intrinsic charm [31].

In addition to the constraints on the gluon nPDF, a large pA dataset will allow quark nPDFs to be constrained, in particular through the aforementioned DY and W/Z measurements both in central and forward/backward regions [44, 47]. It will provide information on sea-quark PDFs, allowing for flavor separation, and access the poorly known strange nPDF. However, in this latter case, much better constraints will be provided by the measurement of the rarer $W+$ charm production [48], which is directly sensitive to the strange quarks in the nucleus, and with sufficient statistics can even provide information on the $s - \bar{s}$ asymmetry. Finally, it should be highlighted that extending the pA program to run with more than one nucleus would allow the study of the nuclear A-dependence of nPDFs, which is very poorly known. Currently, because of the LHC pPb runs, the nPDFs of the lead nucleus are the only ones for which there are constraints for all flavors. For other nuclei that are relatively well studied, such as iron and carbon, only reliable information on up and down (anti)quarks is available. Hence, already having runs with lead and oxygen would make a big impact on our understanding of the nuclear mass dependence of nPDFs. A proton-oxygen run, allowing the measurement of single differential dijet cross sections, would significantly constrain gluons in light nuclei and shed light on its A-dependence [49]. Similarly, detailed pA studies are needed to probe the badly known impact-parameter dependence of nPDFs [50–52].

With regard to studies of TMDs at the LHC, the flagship processes are the Z-boson transverse momentum p_{T} spectra to constrain the quark TMD, and two-particle correlations for color-singlet final states to study the gluon TMD distributions [53–60]. Although the HL-LHC program is essential for a better understanding of the gluon TMDs in the proton, through precise measurements of azimuthal correlations in pp collisions [60], the pA data would help constrain nTMDs, both for quarks and gluons. Currently, the DY process in pPb collisions measured at LHC by CMS [61] and ATLAS [62], together with other available lepton-nucleus data, were used to perform a global fit of the quark nTMD [63]. In addition, experimental constraints of nTMDs will help to match the leading-power TMDs discussed here with the small-x TMDs appearing in the context of gluon saturation (see section 3.3).

3.2. Constraints on proton GPDs and PDFs

UPCs at the LHC serve as an abundant source of high-energy photons making the LHC by far the most energetic photon–proton collider ever [6]. In photoproduction processes in pA collisions, the ion is usually the γ emitter, since the photon flux is proportional to the square of the ion charge, $\phi_{\gamma/A} \propto Z^2$, and this emitted photon acts as a probe of the proton. Compared to pp collisions, pA collisions offer a distinct advantage when probing the nucleon since there is less ambiguity in the identity of the photon emitter (see also [64]). This partly compensates for the lower luminosity. A further benefit is the absence of significant pileup in pA collisions in comparison to pp running, where the superposition of up to 200 collisions per beam crossing in Run 4 makes the identification of photoproduction events almost impossible. Compared to AA collisions in which the *nuclear* PDF is probed, it is the *free*-proton PDF that is probed in pA collisions. Both exclusive and inclusive photoproduction studies are possible, and the quasi-real nature of the photon coherently emitted by the nucleus allows accurate measurements of various distributions related to the proton structure, such as PDFs and GPDs.

Photon-induced measurements in pA UPCs provide access to GPDs in a unique kinematic region different from that of fixed-target experiments (COMPASS, HERMES, JLab), and the upcoming EIC. Final states composed of two photons [65–67], a meson–photon pair [68–71], or a meson–meson pair [72] cover the whole set of unpolarized, polarized, and transversity GPDs with small-ξ reach, and provide complementary observables for the chiral-even sector in deeply virtual Compton scattering and meson production (DVCS and DVMP). Projections for pPb UPCs have been performed for $\gamma\pi^{\pm}$ [70] and $\gamma\rho^{\pm,0}$ [71], resulting in promising anticipated statistics, both in the chiral-even and chiral-odd sectors at moderate ξ, the low-ξ region being more favorable for the chiral-even sector. Collecting $\mathcal{L}_{\text{int}} = 1.2\ \text{pb}^{-1}$ of data in Runs 3 and 4, and ensuring that the square of the γ-meson invariant mass is above $2\ \text{GeV}^2$, about 16 000 $\gamma\rho^0_L$ pairs (1700 $\gamma\rho^0_T$ pairs)[25] are expected to be produced, which probe the chiral-even (chiral-odd) sector of GPDs. With the same integrated luminosity, in the small $5 \times 10^{-5} < \xi < 5 \times 10^{-3}$ range, about 800 $\gamma\rho^0_L$ pairs are expected. By extension, the study of meson-meson pair production at large invariant mass can in addition provide access to the whole set of GPDs, with the practical advantage that a photon is not required to be observed in the final state [72].

Measurements of exclusive quarkonium ($\mathcal{Q}$) photoproduction, $\gamma p \to \mathcal{Q}p$, across multiple collision systems span a broad kinematic range in γ-proton CM energy [73–79], and have been measured in pA and low-luminosity pp collisions at the LHC. Such measurements are necessary for the extraction of GPDs, since these depend on both variables. These measurements extend the coverage provided by HERA and probe much higher CM energies than will be available at the EIC. The HL pPb program offers extended coverage in x and greater statistical precision, particularly for $\psi(2S)$ and Υ measurements [80]. In addition, there are reduced model dependencies in the calculation of the survival factor due to the absence of the two-fold ambiguity of the emitter [81]. The measurements will provide strong constraints on gluon GPDs [82], which are poorly known, and constrain the gluon PDFs via the Shuvaev transform for $Q^2 \approx 2.4$–$22\ \text{GeV}^2$ and $x \approx 3 \times 10^{-6}$–$10^{-3}$ [83–85]. Analyses using J/ψ photoproduction data in pp have already shown the possibility to reduce PDF uncertainties in a previously unexplored kinematic domain [86–88]. The pPb measurements will decrease the theoretical uncertainties and improve the precision with which the PDFs are determined. Furthermore, measurements of higher-mass quarkonia, such as Υ, will provide constraints on the Q^2 evolution in the mid-to-low x domain and test factorization [89], while the $\sigma(\psi(2S))/\sigma(J/\psi)$ cross-section ratio will measure the structure of the radial wavefunction at the origin. To measure the photon PDF of the proton, a new experimental method has been proposed [90], based on the measurement of dilepton production via $\gamma p \to \ell^+\ell^- + X$ in pA collisions.

The t-dependence of J/ψ photoproduction on the nucleus has been measured in PbPb collisions [91], but a cross-section measurement doubly differential in energy and t, for photoproduction on the proton, will only be possible with HL-pA collisions. A fit of the $\gamma p \to J/\psi p$ cross-section as a function of both energy and t will allow a determination of the slope and intercept of the Pomeron trajectory. Such a measurement can also probe the validity of the widely-adopted factorization of the t-dependence in PDF and GPD modelings. Measurements of exclusive J/ψ production in pA collisions can also look for higher-twist GPD contributions by testing s-channel helicity conservation through measurements of the meson polarization. First measurements have been performed in PbPb collisions [92], but more data are required to perform the test in pA collisions.

Besides the exclusive processes discussed above, UPCs can also lead to inclusive photoproduction processes. To date, inclusive UPCs have been only measured in PbPb collisions

[25] Here, ξ is the longitudinal momentum asymmetry between the initial and final states.

looking for dijet [93, 94] and charm [95] photoproduction. Inclusive quarkonium photoproduction has been shown [96] to be measurable by the four LHC experiments in pPb UPCs, and would increase the p_{T} reach of the HERA data [97–99] from 10 to 20 GeV and even of the future EIC [100]. Similarly, dijet, charm, bottom inclusive photoproduction, to name a few, will be accessible in pPb UPCs and will improve the determination of the low$-x$ gluon PDFs of the proton. In addition, the corresponding J/ψ, Υ, and $\psi(2S)$ spectra, particularly at large p_{T}, would discriminate better among different production mechanisms compared to single inclusive hadroproduction data in pp at the HL-LHC. Finally, the p_{T} spectrum of non-prompt J/ψ photoproduction is also measurable, probing bottom photoproduction and improving the interpretation of the HERA J/ψ data. Measurements of J/ψ dissociative photoproduction are sensitive to shape fluctuations of the proton [101], in particular to energy-dependent gluonic hot spots, which should be increasingly suppressed at high energies [102]. The ALICE forward calorimeter (FoCal) [103, 104] is particularly suited to directly test this phenomenon in pPb collisions [105]: a dissociative J/ψ cross section falling with CM energy would signal the onset of nonlinear QCD effects.

3.3. Small-x QCD and gluon-saturation physics

The phenomenon of gluon saturation arises from the nonlinear nature of QCD at high energies [106–109], and manifests itself as a breaking of the DGLAP-based description of PDFs [110, 111]. It is expected that a hadronic target is found in a saturated state, when a probe (quark or gluon) scatters off a small-x gluon constituent, with $x \lesssim 10^{-4}$. Due to the nonlinear effects, a dynamical saturation scale $Q_s(x)$ is generated, which is further enhanced by the target mass number, roughly $Q_s^2(x) \sim A^{1/3}$ for large nucleus [5, 112–114]. Therefore, direct searches for gluon saturation are best performed through scattering off heavy nuclei, and measuring forward particle production observables, using pp collisions as a reference.

A suppression of the forward pA cross sections (per nucleon) compared to pp was observed at RHIC, both for inclusive hadron production and two-particle correlations [115–119], and at the LHC in the inclusive hadron p_{T} spectra measured by LHCb [120, 121]. While qualitatively consistent with the saturation picture, the Color Glass Condensate (CGC) theory for saturation predicts less suppression than observed [122]. Indirectly, nonlinear effects may be visible [123] in J/ψ photoproduction on the nuclear target in PbPb UPCs by ALICE and CMS [124–126] compared to results on the proton target [77, 78, 127, 128]. On the other hand, the data [124] cannot distinguish between saturation [129–131] and non-saturation models. Similarly, the comparison of dijet correlations in the ATLAS forward rapidity for pPb and pp [132] seems to suggest a subtle interplay of nonlinear effects and perturbative Sudakov resummation [133], although subject to large experimental and theoretical uncertainties. Finally, the forward inclusive jet energy deposit in pPb collisions measured by CMS in the CASTOR detector [134] seems to challenge both the theoretical descriptions based on saturation [135–137], as well as the available Monte Carlo event generators.

In view of the above, a dedicated pA LHC program is crucial in disentangling the different effects and finding clear evidence for nonlinear evolution in nuclei. Since one of the essential predictions of the gluon saturation models is the collective behavior of gluons (carrying average transverse momenta $k_{\mathrm{T}} \sim Q_s$), the most significant observables are related to azimuthal particle correlations at forward rapidities. The CGC theory predicts a sensitivity of the initial-state target to the color flow in the final state. Therefore, one of the crucial measurements is of azimuthal correlations for various final states in a broad transverse momentum range, including photoproduction on a nuclear target in UPCs. From a theoretical viewpoint,

Table 2. Impact of the two basic small-x TMD gluon distributions to various processes accessible in HL proton-nucleus collisions at the LHC (adapted from [138]).

TMD type	Hadron in pA	Photon-jet in pA	Dijet in γA (AA UPC)	Dijet in pA
WW	✗	✗	✓	✓
dipole	✓	✓	✗	✓

the simplest two-particle correlations sensitive to saturation are photon-jet and photon-hadron correlations in pPb collisions at large $|\eta|$. The cross section depends on a single non-perturbative TMD small-x gluon field correlator, called the dipole gluon distribution, which is also accessible in inclusive DIS [138] (see [139–142] for phenomenological predictions). Photon-jet correlations can be accessed up to $\eta \approx 5.1$, in the planned FoCal calorimeter of ALICE, in LHCb, and up to $|\eta| = 4$ in ATLAS and CMS at HL-LHC. In addition to the dipole TMD gluon distribution, the description of small-x phenomena in the saturation regime requires other types of TMD gluon distributions [138, 143]. The Weizsäcker–Williams (WW) distribution, used in the leading-power TMD factorization formalism [144], can be directly probed at the LHC in dijet correlations in UPC photoproduction on a nuclear target [145–147], which would complement similar future measurements performed at EIC [148]. Table 2 summarizes the impact of the two basic small-x TMD distributions to different processes accessible at HL-LHC. In particular, the precise measurement of dihadron and dijet correlations in pPb collisions at forward rapidity [149, 150], as well as transverse energy-energy correlators [151], will provide stringent theory tests.

Exclusive photoproduction of light mesons with a rapidity gap can help discriminate between the non-saturation (à la BFKL) and saturation (CGC) scenarios by exploiting their different t dependence. Exploring the entire spin density matrix should provide a large set of observables [152–156], giving access to the generalized TMDs (GTMDs) of the proton. Single [157] and double [158] hadron photoproduction processes are also sensitive to GTMDs, but single inclusive observables will remain important. Last but not least, a full understanding of low-x dynamics will require more direct observables of the intermediate region of high gluon density targets, where the low-x linear BFKL energy evolution is needed, but saturation is not relevant yet. In particular, despite there being indirect experimental evidence for the Odderon in elastic pp scattering [159], there are no experimental hints of the Odderon in the hard sector. To address this, pA collisions provide good prospects for observation through interference effects in exclusive $\pi^+\pi^-$ photoproduction [160]; by the observation of $C=+1$ parity mesons in photoproduction [161]; and through the transverse momentum distribution of exclusive J/ψ mesons [162].

3.4. Benchmark for QGP physics and onset of parton collectivity

One of the main motivations for studying pA collisions at the LHC was to obtain a reliable baseline, without final-state effects, to interpret the AA-collision results. However, with the rising interest in parton collectivity in small systems (e.g. in the creation of QGP in pPb collisions) the pA program itself merits dedicated study. Historically, pA collisions at the LHC and RHIC were mainly motivated by measuring the so-called 'cold' nuclear matter effects on strongly interacting probes of the QGP. Their main purpose was to measure how the production of such probes was suppressed by the modification of the nuclear partonic densities,

by initial-state energy loss, and/or by final-state interactions [163]. The *pA* runs have proven to be absolutely essential as they uncovered a variety of unexpected effects that need to be understood in their own right, as well as being crucial for the interpretation of *AA* measurements. In particular, the observations of azimuthal correlations that are long-range in rapidity, are indicative of collective behavior in high multiplicity *pp* [164] and *p*Pb [165–167] collisions. This observed collectivity in small systems has triggered intensive research [4, 168] to understand its origins. Explanations range from strong final-state effects similar to *AA* collisions, to initial-state effects due to gluon saturation, while the success of hydrodynamic models in describing the *p*Pb data calls for further research. High luminosity *p*Pb collisions also provide a unique opportunity to study complex vortex-like structures in QGP droplets; for example, studies of hyperon polarization could lead to the discovery of the toroidal vorticity in nuclear matter [169, 170]. Therefore, while more detailed *pA* studies of cold nuclear matter effects, e.g. the relative suppression of excited quarkonia compared to their ground states in *p*Pb collisions, are needed, a HL-*pA* run at the LHC will also provide much further information on the origins of parton collectivity.

3.5. Double and triple parton scatterings

Double and triple parton scattering (DPS and TPS) processes in high-energy hadron–hadron collisions open up novel opportunities to investigate the partonic hadron structure [171–174], and complement the multidimensional picture of hadrons as described by GPDs and TMDs. In addition, DPS and TPS final states constitute backgrounds for BSM searches (see e.g. [175]). Although the DPS and TPS signals are typically much smaller than the equivalent signal produced in single parton scattering (SPS) processes, they can be enhanced by extending the transverse size of one of the colliding hadrons using heavy nuclear targets[26] [177–181], whereas they are completely swamped by binary-scaling contributions from different nucleon–nucleon scatterings in *AA* collisions [176, 182]. Multiple experimental analyses of DPS have been performed, whose results are usually summarized through the extraction of the so-called effective cross section, $\sigma_{\rm eff}$, defined as the normalized ratio of SPS to DPS cross sections for the same final states. This quantity provides critical insights into the transverse hadron structure, and badly known double parton correlations [174]. In a purely geometric approach, $\sigma_{\rm eff}$ is assumed to be a process-independent constant [176, 183], although recent compilations of measurements show differences between $\sigma_{\rm eff}$ extracted from processes involving quarkonium [184–189] and jets or gauge-boson production [190]. Parton correlations might explain these discrepancies, which can be better investigated with HL-*p*Pb data.

Estimates for DPS and TPS contributions to heavy-quark, quarkonium and/or electroweak pair production in *p*Pb collisions at the LHC have been provided in [181, 191]. To date, only two experimental extractions of $\sigma_{\rm eff}$ exist in *p*Pb collisions from double charm mesons [192] and double J/ψ [190] production. Both measurements are statistically limited and more data are required. A clean extraction of $\sigma_{\rm eff}$ is possible from same-sign W boson production [179], where a few pb^{-1} of data would allow a precision of 10%. A comprehensive investigation of DPS in gluon-initiated processes is possible through $J/\psi + \Upsilon$ production [7]. Currently, only a limited number of events have been observed by CMS in *pp* collisions, and the use of Pb nuclei would increase the corresponding rate. Moreover, double-Υ production would enable a comparative analysis of the extracted $\sigma_{\rm eff}$ with that obtained in double-J/ψ production,

[26] In *p*Pb collisions ($A = 208$), DPS and TPS yields are enhanced by factors of about $3 \times A$ and $9 \times A$ compared to *pp* collisions [176].

providing insights into the role of final-state interactions. Finally, large data samples are needed to carry out multidifferential studies of σ_{eff}, e.g. as a function of difference in rapidities or azimuthal angles between final states [193, 194]. These analyses will provide unique information on double-parton correlations that cannot be accessed otherwise. The separation of DPS from SPS processes can also be facilitated in *pA* collisions by exploiting their different centrality dependence [195].

A more detailed understanding of DPS can be achieved through the study of TPS in *pp* [176] and *p*Pb [196] collisions. In *pp*, TPS has been searched for in triple J/ψ production [184], and also in this case, the rate will be enhanced in *p*Pb collisions. Large data samples offer unique opportunities to observe TPS, e.g. in $\phi\phi D$ or $\phi\phi J/\psi$ production. Note that in *pp* (*p*Pb) collisions, triple charm production is almost 15 (20)% of all inclusive charm production, so not only can the role of TPS not be neglected, but it is mandatory to properly characterize the corresponding final states [176]. Another promising channel is 6-jet production, where the impact of TPS can be up to 20% of the total cross section above a jet transverse momentum, $p_{\text{T}}^{\text{jet}} \approx 20$ GeV in *pp* collisions, an effect that is further increased in the *p*Pb case [197].

3.6. Production and spectroscopy of bound states

In the quarkonium sector, LHCb has measured multiple states in *p*Pb collisions [198], covering a broad range of binding energies and sizes. After accounting for initial-state effects, the data reveal a trend of dissociation of quarkonium states with weak binding, such as $\psi(2S)$, and production consistent with scaled *pp* collisions for states with binding energy larger than 180 MeV. The exceptions are prompt $\Upsilon(2S)$ and $\Upsilon(3S)$ states, which show anomalous suppression relative to the $\Upsilon(1S)$ yields [199]. The potential cause of these suppressions is the feed-down contribution of weakly bound χ_b states [200]. However, χ_b states were never measured in *p*Pb collisions due to the low efficiency for low-energy photons produced in the decay $\chi_b \to \Upsilon + \gamma$, and more data are required. Multiplicity-dependent measurements of $\chi_c \to J/\psi + \gamma$ states to search for anomalous suppression in high-density events, as well as measurements of the $\chi_b \to \Upsilon + \gamma$ feed-down contributions are essential to confirm the origins of $\Upsilon(2S)$ and $\Upsilon(3S)$ anomalous suppression. The challenging observation of the η_c state will only be possible at high luminosity and will allow a better understanding of the behavior of color-singlet states in the nuclear medium.

In the field of exotic hadrons, 75 new hadrons have been discovered at the LHC to date [201] including many combinations of (candidate) tetraquark and pentaquark states. The nature of a large number of these exotic hadrons is still under debate as it is not clear whether they are tightly bound or molecular-like. Their binding and configuration are still largely unknown, and so *pA* collisions function as an excellent laboratory to study their properties. Of particular interest is to understand how these exotic states are produced and interact in high-density environments. LHCb observed an enhancement of tetraquark-candidate $\chi_{c1}(3872)$ production in *p*Pb compared to *pp* collisions [202], hinting at the role of statistical hadronisation in their formation, where the larger number of initial-state quarks increase the probability of multiquark hadron production [203]. High-luminosity *p*Pb collisions can provide more precise measurements of $\chi_{c1}(3872)$ and other exotic hadrons, including their density-dependent production and 'destruction'. One expects a trade-off between statistical-hadronisation formation and dissociation of weakly-bound exotic states by comoving particles [204], depending on their microscopic nature. Exotic production from intrinsic charm [205] can also be searched for in HL-*p*Pb collisions, where the asymmetric collision can isolate charm-rich partonic environments at large x.

3.7. Photon–photon collisions

Both LHC protons and heavy ions can act as sources of initial-state photons and hence photon–photon collisions occur abundantly in UPCs at the LHC [6]. Being a color-singlet exchange, $\gamma\gamma$ collisions naturally lead to events with intact projectiles and rapidity gaps in the final state. Together with low-pileup conditions, UPCs give very clean experimental signatures with very few particles registered in a detector. The photon flux accompanying each beam is proportional to Z^2, thus, cross sections for $\gamma\gamma$ processes are significantly enhanced in AA compared to pA and pp collisions. While the $\gamma\gamma$ luminosities in pA collisions are overall reduced by a factor Z^2 compared with the AA case, the proton beam energies are larger, and the associated photon fluxes are much harder, than in PbPb UPCs. As a result, the pA collisions probe significantly larger $\gamma\gamma$ CM energies [206], and they are also useful to resolve discrepancies between pp and AA UPCs. Already some hints of mild deviations [207–209] between data and LO predictions exist for exclusive e^+e^- and $\mu^+\mu^-$ production, that highlight the need for a proper modeling of inelastic contributions [210] as well as of the Pb photon flux and higher order QED corrections [211]. Additional datasets with the asymmetric $\gamma\gamma$ collisions provided by pA UPCs can help clarify all these aspects. Also, particular UPC processes possible in the pA mode, such as single-W photoproduction [212], require large data samples. Forward neutron production from electromagnetic ion dissociation has gained interest in AA UPCs [207, 208, 213–216] and is increasingly used in online and offline event selection of SM processes, as well as in BSM searches [217]. Different neutron multiplicities have different impact-parameter profiles that lead to modifications of central kinematics. The simplicity of dilepton production in the pA system, which constrains neutron emission from just one nucleus, will improve the modeling of dissociation for the AA system.

3.8. Beyond the standard model

At face value, pA cannot compete with pp collisions at the LHC in terms of the production of heavy BSM objects, as they have lower CM energies and integrated luminosities. However, akin to the AA case [218, 219], pA collisions feature $\gamma\gamma$ interactions without pileup and with large photon fluxes (from the Pb side) that partially compensate for these drawbacks (provided that a large $\mathcal{L}_{\rm int}$ is achieved) for photon-coupled BSM objects. In terms of attainable $\gamma\gamma$ luminosity, the HL-pPb mode would outperform the PbPb UPCs reach in the $m_{\gamma\gamma} \approx 50$–$300$ GeV mass range [206]. This is relevant e.g. to set competitive limits on heavy axion-like particles [220].

In order to compare the generic BSM reach of pA with pp and AA collisions, we introduce a simple ansatz for the $\gamma\gamma$ collision cross section: $\sigma_{\gamma\gamma}(n) \propto s_{\gamma\gamma}^{n-1}/\Lambda^{2n}$. This simplified cross section encodes the CM energy ($\sqrt{s_{\gamma\gamma}}$) dependence, which is one of the key elements to compare the collision modes. In a specific model, the Λ parameter would generally encapsulate a combination of couplings and masses. This simplified approach provides a rough classification of BSM candidates as a function of n. The value $n = 0$ includes SM-like processes (see e.g. [221]), $n = 1$ includes resonant effective field theories (EFTs) (see e.g. [222, 223]), and $n \geqslant 2$ arises from non-resonant EFTs, such as F^4 operators [224] and continuum EFTs [225, 226]. Using this approach, we classify the BSM scenarios to be searched for in UPCs into (roughly) two types: low-mass resonances and non-resonant EFTs.

The low-mass resonances[27] are described by resonant EFTs. In that case, we obtain that the pPb mode competes with the pp mode. The non-resonant EFTs include anomalous quartic

[27] UV motivated CP-odd resonances include the PQ axion [227, 228], stringy axions [229–234], and Goldstone bosons [235], whereas CP-even resonances include the radion [236], dilaton [237], composite radial mode [238, 239], extended Higgs sectors [240], Higgs portal [241], and KK gravitons [224, 242].

gauge couplings[28] and continuum EFTs[29]. In that case, we obtain that *p*Pb competes with *pp* with an event yield only moderately smaller, but with a much cleaner selection due to reduced pileup. Due to this complementarity, assuming no prejudice on the type of BSM scenario, searches using HL-*p*Pb collisions provide a useful strategy to maintain sensitivity over the broadest range of new physics possibilities. More detailed studies of effective operator searches in *p*Pb would be useful to reinforce such a conclusion.

3.9. Ultra high-energy cosmic-ray physics

Cosmic rays, ranging from medium to ultra-high energies, originate from various astrophysical sources and produce extensive air showers (EAS) upon interaction with atmospheric nuclei. These showers provide valuable information about the primary particles, including their mass composition and energy spectrum. The study of cosmic rays and EAS offers a unique opportunity to probe the behavior of strongly interacting matter under extreme conditions, provided that the hadronic interaction models reproduce the *pA* collider data up to the highest possible energies [8, 258]. The analysis of EAS has highlighted challenges, notably the 'muon puzzle' [259, 260], whereby current hadronic interaction models fail to accurately predict muon production for a given primary mass [261]. An improved description of the EAS data requires significant changes to the models, both for their predicted position of the shower maximum and for the fraction of signal at ground associated to the number of muons [262]. This discrepancy suggests an incomplete understanding of hadronic interactions at ultrahigh energies and has sparked interest in exploring new phenomena, in particular linked to nuclear effects in small systems [263]. As a matter of fact, one of the sources of the 'muon puzzle' is seemingly the presence of *pA* collisions that do not behave as a simple superposition of *pp* interactions [264]. Similarly, another area where more LHC *pA* data are welcomed is in the interpretation of ultrahigh-energy astrophysical neutrinos as measured by the IceCube experiment [265, 266]. A background to cosmic neutrinos comes from atmospheric neutrinos produced in cosmic-ray interactions with air nuclei. The HL-*pA* data can provide more precise information on the production of forward charmed particles, which are important to constrain this background [267].

4. Summary and conclusions

High-energy proton-nucleus collisions (*pA*) provide a bridge between proton-proton (*pp*) and ion-ion (*AA*) collisions with two particular merits: firstly, the asymmetric projectiles and beam energies ensure that effects associated with the proton can be distinguished from those of the nucleus; secondly, a path towards understanding the complexity of two large systems of colliding bound nucleons is provided through the interaction of a well-understood proton on the complex ion.

At the LHC, a few weeks of *pA* collisions were performed in Runs 1 and 2 in a diversity of operating conditions, and have already brought essential contributions to particle, heavy-ion, and cosmic-ray physics, leading to the discovery of new phenomena as well as the confirmation and extension of effects discovered in lepton-nucleus collisions. Multi-TeV *pA* collisions offer several unique physics opportunities:

[28] UV motivation includes heavy neutral particles linearly coupled to the SM [224, 243], new charged particles [221, 243], polarizable dark particles [239] and Born-Infeld QED [244–246].
[29] UV motivation includes AdS [247–251], linear dilaton [225, 226, 252, 253] and other braneworld geometries [254], and strongly-interacting dark sectors [255–257].

Table 3. Qualitative comparison of various experimental setups with respect to different physics observables. An increasing number of star points indicates a better environment for the considered physics topic.

Physics topics\collider	EIC	FT@LHC	HL-*pA*@LHC	*pp*@HL-LHC	*AA*@HL-LHC
PDFs	⋆⋆⋆⋆	⋆⋆⋆	⋆⋆	⋆⋆⋆	—
nPDFs	⋆⋆⋆⋆	⋆⋆⋆	⋆⋆⋆	—	⋆⋆
TMDs	⋆⋆⋆	⋆⋆⋆	⋆⋆⋆	⋆⋆	—
nTMDs	⋆⋆⋆	⋆⋆	⋆⋆	—	⋆
GPDs	⋆⋆⋆	⋆	⋆⋆	⋆	—
nGPDs	⋆⋆⋆	⋆	⋆	—	⋆⋆
Parton saturation searches	⋆⋆⋆	⋆	⋆⋆⋆⋆	⋆⋆⋆	⋆⋆⋆
Odderon searches	⋆⋆	⋆	⋆⋆⋆	⋆⋆	⋆⋆
Parton collectivity	—	⋆⋆⋆	⋆⋆⋆	⋆⋆	⋆⋆⋆⋆
DPS/TPS	⋆	⋆	⋆⋆⋆⋆	⋆⋆⋆⋆	⋆
Hadron spectroscopy	⋆	⋆	⋆⋆⋆	⋆⋆⋆	⋆⋆
BSM searches	⋆	⋆	⋆⋆	⋆⋆⋆⋆	⋆⋆

- They provide a way to study nuclear modifications to PDFs and cold nuclear matter effects (such as shadowing, parton saturation, and energy loss) without the complexities of hot QCD medium effects present in *AA* collisions.
- They serve as a crucial reference for disentangling initial-state nuclear effects from final-state medium effects in *AA* collisions, aiding in the interpretation of QGP signatures.
- They typically achieve higher luminosities than *AA* collisions and much reduced pileup compared to *pp* collisions, enabling more precise measurements.
- They provide a unique platform to extend studies of small-x QCD and gluon saturation by probing smaller momentum fractions than any other current experimental setup.
- They offer valuable insights into the interplay of enhancement and suppression mechanisms in nuclear matter and a cleaner environment to study coalescence and fragmentation in hadronisation.
- They are essential for the modeling of high-energy cosmic-ray and neutrino interactions, providing a link between particle physics and astrophysics.

The physics potential provided by the proton and heavy-ion LHC beams in asymmetric *pA* collisions offers multiple complementarities and advantages compared to *pp* and *AA* collisions. We have summarized the physics case for a high-luminosity *pA* run (HL-*pA*@LHC) under twelve research axes, where large data samples are required to reduce the current experimental uncertainties and/or to study (for the first time) multiple rare processes of interest. Table 3 gathers qualitative comparisons of the impact that *pA* can have on each of these physics topics, with respect to other collision scenarios: EIC [36], FT@LHC [35], *pp*@HL-LHC [268], *AA*@HL-LHC [14]; with ⋆ symbols assigned as explained below.

Regarding

- PDF studies, the best experimental setup is given by the future EIC with cleaner probes and access to polarized PDFs, while *pp*@HL-LHC and FT@LHC complement its reach by probing the low-x and large-x regimes, especially in the gluon sector. HL-*pA*@LHC can contribute in a timely manner to gluon PDF studies via inclusive photoproduction

($Q^2 \simeq 0$) in UPCs with a significantly wider range in transverse momentum and γ-proton CM energy than at HERA, and with indirect PDF constraints via exclusive $\mathcal{Q}$ photoproduction.

- nPDF studies, the best setup is the EIC as an *eA* collider with cleaner final states. However, HL-*pA*@LHC covers much lower x, while FT@LHC offers access to larger x with more versatility in the probed nuclei, and earlier than the EIC. The *AA*@HL-LHC program offers some sensitivity on nPDFs if the additional hot nuclear effects can be separated out.
- TMD studies, the best setups are the future EIC, FT@LHC, and HL-*pA*@LHC for very different reasons. On the one hand, FT@LHC would benefit from the possibility to polarize the target for single transverse-spin asymmetries studies of gluon-sensitive probes, which are essentially unknown. The EIC will profit from both beams and target polarizations and from cleaner probes. On the other hand, HL-*pA*@LHC can study TMDs in the low-x regime in the dense-dilute limit, which cannot be accessed otherwise, as well as potentially via azimuthal asymmetries in inclusive photoproduction. Lastly, *pp*@HL-LHC can also definitely help in probing TMDs at low x via azimuthal asymmetries but kinematical cuts due to triggers are usually very harmful.
- nTMD studies, the best setup is the future EIC as an *eA* collider that can access a large variety of TMD-factorisable processes. The FT@LHC and HL-*pA*@LHC programmes can access nTMDs via DY final states. Whereas *AA*@HL-LHC can in principle measure nTMDs via azimuthal asymmetries in photoproduction (UPCs), the event counts are expected to be very small.
- GPD studies, the best setup is the EIC with polarized beams, while HL-*pA*@LHC via UPCs offers very interesting possibilities through exclusive-photoproduction channels such as timelike Compton scattering, or with large final-state invariant-mass systems in meson-pair or photon-meson photoproduction. Similar exclusive final states can be studied at *pp*@HL-LHC but would be 'polluted' by hadronic exchanges.
- nGPD studies, the best setup is the EIC via *eA* exclusive reactions that can be complemented at *AA*@HL-LHC by exclusive-$\mathcal{Q}$ photoproduction reactions via UPCs. HL-*pA*@LHC has a limited sensitivity to nGPDs with the same observable in the rapidity region where the probability for photon emission by the proton becomes significant. Finally, at FT@LHC in PbA UPCs, the nGPDs of various nuclear targets could also be probed via exclusive-$\mathcal{Q}$ photoproduction.
- parton-saturation searches, the best setup is the HL-*pA*@LHC via forward hadron and jet production processes and their correlations. At *AA*@HL-LHC, saturation can be studied via several UPC observables while *pp*@HL-LHC is needed both as a reference for saturation studies in nuclei and to test the need for the small-x resummation. While the future EIC will study inclusive and exclusive processes sensitive to saturation in *eA* collisions, the forward detector upgrades of the LHC experiments will allow probing the partonic structure of heavy nuclei at much smaller x. Diffractive processes in UPCs are particularly promising since their extended kinematics offers a bridge towards GTMD studies.
- odderon searches, the best setup is the HL-*pA*@LHC through the observation of $C = +1$ mesons (or meson pairs, e.g. $\pi^+\pi^-$) photoproduction, which is sensitive to interferences of $C = +1$ (pomeron) and $C = -1$ (odderon) exchanges. Such processes are also possible at the EIC, but require very high luminosity. Good prospects are also present in UPCs at *AA*@HL-LHC if the photon emitter can be identified.
- parton-collectivity studies, the best setup is the *AA*@HL-LHC as a laboratory for QGP creation. FT@LHC via Pb*A* collisions can study collectivity in a complementary rapidity

and (lower) energy domain. However, HL-pA@LHC, and to a lesser extent pp@HL-LHC, can provide new probes of the generation of collective partonic behavior in small systems.

- DPS/TPS studies, the best setups are HL-pA@LHC (thanks to the $3 \times A$ and $9 \times A$ enhanced yields, respectively, for pPb compared to pp collisions) and pp@HL-LHC (thanks to its very large integrated luminosity and higher $\sqrt{s}$, enabling the production of pairs of very heavy particles) with large rates for multiple DPS/TPS processes. These provide access to novel information on the partonic structure that cannot be obtained elsewhere. HL-pA@LHC will facilitate the determination of the effective cross section as a function of multiple kinematic variables, hence revealing previously unexplored multiparton correlations.
- hadron spectroscopy, the best setups are HL-pA@LHC and pp@HL-LHC. The latter has allowed the identification of a great number of exotic states, while the former is important in elucidating their nature by exploiting their density-dependent production and final-state interactions.
- BSM searches, the best setup is pp@HL-LHC, while both HL-pA@LHC and AA@HL-LHC UPCs provide a clean environment for low- and intermediate-mass photon-coupled BSM objects, such as new even-spin particles. In UPC searches for low-mass resonances, pPb competes with PbPb in sensitivity, whereas in UPC searches for non-resonant EFTs, pPb has slightly lower yield than pp but cleaner selection due to reduced pileup. Due to this complementarity, assuming no prejudice on the type of the BSM scenario, searches using HL-pPb collisions can provide a strategy to maintain sensitivity over the broadest range of new physics possibilities.

It appears clear from the above that the allocation of dedicated pA-collision run(s) at the LHC will provide unique physics inputs complementary to those offered by other major existing or planned facilities. We therefore strongly encourage additional pA running at the LHC in Runs 3 and 4, in order to achieve and extend the original physics targets in a timely manner, and to provide the data for the many important measurements summarized in this document.

Acknowledgments

This work has received funding from the French CNRS via the IN2P3 projects 'QCDFactorisationAtNLO' and the COPIN-IN2P3 project #12-147 'kT factorization and quarkonium production in the LHC era', via the ANR under the grant ANR-20-CE31-0015 ('PrecisOnium'), by the Paris-Saclay U. via the P2I Department and by the GLUODYNAMICS project funded by the 'P2IO LabEx (ANR-10-LABX-0038)' in the framework 'Investissements d'Avenir' (ANR-11-IDEX-0003-01) managed by the Agence Nationale de la Recherche (ANR), France. The material presented has been based upon work supported also by the U.S. Department of Energy, Office of Science, Office of Nuclear Physics, under DOE Contract No. DE-SC0012704 and within the framework of the Saturated Glue (SURGE) Topical Theory Collaboration. The research conducted in this publication was funded by the Irish Research Council under grant number GOIPG/2022/478 and the Joint PhD Program of Université Paris-Saclay 1248 (ADI). A.K. acknowledges the support of the Polish Narodowe Centrum Nauki under Sonata Bis Grant No. 2019/34/E/ST2/00186. I.G.-B. and P.K. were supported by the programme 'Excellence initiative - research university' for the AGH University of Krakow, grant no 9722. C.V.H. has received funding from the programme 'Atracción de Talento', Comunidad de Madrid (Spain), under the grant agreement No 2020-

T1/TIC-20295. LHL thanks the Science and Technology Facilities Council (STFC) part of U.K. Research and Innovation for support via the grant award ST/T000856/1. F.J. has been supported by the US Department of Energy. The work of L.S. was supported by the Polish Narodowe Centrum Nauki, Grant No. 2024/53/B/ST2/00968 . The research of M.S. was supported by the US Department of Energy Office of Science, Office of Nuclear Physics under Award No. DE-FG02-93ER40771. The research of DTT was supported by the U.S. Department of Energy Office of Science, Office of Nuclear Physics. E.G.F acknowledges the support of the Spanish Research State Agency under project PID2023152762NB-I00 supported by MCIU/AEI/10.13039/501100011033/FEDER,EU. A workshop was supported by EU Horizon 2020 research and innovation programme under STRONG-2020 grant agreement No. 824093.

Data availability statement

No new data were created or analyzed in this study.

References

[1] Jowett J and Carli C 2006 The LHC as a proton nucleus collider *Conf. Proc. C* **060626** 550–2 Proc. of the European Particle Accelerator Conf. 2006, Edinburgh, Scotland, https://accelconf.web.cern.ch/e06/PAPERS/MOPLS009.PDF
[2] Salgado C A *et al* 2012 Proton-nucleus collisions at the LHC: scientific opportunities and requirements *J. Phys. G* **39** 015010
[3] Klasen M and Paukkunen H 2024 Nuclear PDFs after the first decade of LHC data *Ann. Rev. Nucl. Part. Sci.* **74** 49–87
[4] Grosse-Oetringhaus J F and Wiedemann U A 2024 A decade of collectivity in small systems arXiv:2407.07484
[5] Jalilian-Marian J and Kovchegov Y V 2006 Saturation physics and deuteron-gold collisions at RHIC *Prog. Part. Nucl. Phys.* **56** 104–231
[6] Baur G *et al* 2008 The physics of ultraperipheral collisions at the LHC *Phys. Rept.* **458** 1–171
[7] Chapon E *et al* 2022 Prospects for quarkonium studies at the high-luminosity LHC *Prog. Part. Nucl. Phys.* **122** 103906
[8] d'Enterria D, Engel R, Pierog T, Ostapchenko S and Werner K 2011 Constraints from the first LHC data on hadronic event generators for ultra-high energy cosmic-ray physics *Astropart. Phys.* **35** 98–113
[9] Brüning O *et al* 2004 LHC design report v.1: the LHC main ring *CERN-2004-003-V1* CERN, Geneva, Switzerland (https://doi.org/10.5170/CERN-2004-003-V-1)
[10] Jowett J *et al* 2013 Proton-nucleus collisions in the LHC *Proc. 4th Int. Particle Accelerator Conf., IPAC13, Shanghai, China, MOODB201* https://cds.cern.ch/record/1572994
[11] Versteegen R *et al* 2013 Operating the LHC off-momentum for *p*-Pb collisions *Proc. 4th Int. Particle Accelerator Conf., IPAC13, Shanghai, China, TUPFI041* http://accelconf.web.cern.ch/AccelConf/IPAC2013/papers/tupfi041.pdf
[12] Jowett J *et al* 2017 The 2016 proton-nucleus run of the LHC *Proc. 8th Int. Particle Accelerator Conf. 2017, Copenhagen, Denmark* (https://doi.org/10.18429/JACoW-IPAC2017-TUPVA014)
[13] Jebramcik M 2019 Beam dynamics of proton-nucleus collisions in the Large Hadron Collider *PhD thesis* Johann Wolfgang Goethe-Universität, Frankfurt am Main, Germany http://cds.cern.ch/record/2724830?ln=en
[14] Citron Z *et al* 2019 Report from Working Group 5: future physics opportunities for high-density QCD at the LHC with heavy-ion and proton beams *CERN Yellow Rep. Monogr.* **7** 1159–410
[15] Bruce R, Alemany-Fernández R, Bartosik H, Jebramcik M, Jowett J and Schaumann M 2021 Studies for an LHC pilot run with oxygen beams *Proc. 12th Int. Particle Accelerator Conf. (IPAC'21): Campinas, Brazil, May 2021* pp 53–6

[16] Bruce R *et al* 2020 HL-LHC operational scenario for Pb–Pb and p-Pb operation CERN-ACC-2020-0011https://cds.cern.ch/record/2722753
[17] D'Andrea M *et al* 2024 Operational performance of crystal collimation with 6.37*Z* TeV Pb ion beams at the LHC *Phys. Rev. Accel. Beams* **27** 011002
[18] Jebramcik M and Jowett J 2019 Moving long-range beam–beam encounters in heavy-ion colliders *Proc. 10th Int. Particle Accelerator Conf. (IPAC'19), Melbourne, Australia, 19–24 May 2019* pp 488–91
[19] Bruce R, Jowett J M, Blaskiewicz M and Fischer W 2010 Time evolution of the luminosity of colliding heavy-ion beams in BNL Relativistic Heavy Ion Collider and CERN Large Hadron Collider *Phys. Rev. Spec. Top. Accel. Beams* **13** 091001
[20] Bruce R, Jebramcik M A, Jowett J M, Mertens T and Schaumann M 2021 Performance and luminosity models for heavy-ion operation at the CERN Large Hadron Collider *Eur. Phys. J. Plus* **136** 745
[21] Bruce R 2024 Proton-nucleus collisions at the LHC: the machine point-of-view, tech. rep., Workshop on Physics with high luminosity proton-nucleus collisions at the LHC https://indico.cern.ch/event/1389579/contributions/5993228/
[22] Arduini G *et al* 2024 LHC upgrades in preparation of run 3 *J. Instrum.* **19** P05061
[23] (ATLAS Collaboration) 2021 Expected tracking and related performance with the updated ATLAS Inner Tracker layout at the High-Luminosity LHC *Tech. Rep. ATL-PHYS-PUB-2021-024* CERN, Geneva https://cds.cern.ch/record/2776651
[24] Rossi A and (CMS Collaboration) 2023 The CMS Tracker for the High Luminosity LHC *Tech. Rep. CMS-CR-2022-091* CERN, Geneva https://cds.cern.ch/record/2816248
[25] (ALICE Collaboration) 2024 Technical Design Report of the ALICE Forward Calorimeter (FoCal) *Tech. Rep. CERN-LHCC-2024-004* CERN, Geneva https://cds.cern.ch/record/2890281
[26] (CMS Collaboration) 2020 The CMS Precision Proton Spectrometer at the HL-LHC—Expression of Interest *Tech. Rep. CERN-CMS-NOTE-2020-008* CERN, Geneva arXiv:2103.02752
[27] (ALICE Collaboration) 2022 Letter of intent for ALICE 3: a next-generation heavy-ion experiment at the LHC arXiv:2211.02491
[28] Jebramcik M and Jowett J 2019 Prospects for future asymmetric collisions in the LHC *Proc. 10th Int. Particle Accelerator Conf. (IPAC'19), Melbourne, Australia, 19–24 May 2019* pp 484–7
[29] Hirai M, Kumano S and Nagai T H 2007 Determination of nuclear parton distribution functions and their uncertainties in next-to-leading order *Phys. Rev. C* **76** 065207
[30] de Florian D, Sassot R, Zurita P and Stratmann M 2012 Global analysis of nuclear parton distributions *Phys. Rev. D* **85** 074028
[31] Stavreva T, Schienbein I, Arleo F, Kovarik K, Olness F, Yu J Y and Owens J F 2011 Probing gluon and heavy-quark nuclear PDFs with $\gamma + Q$ production in pA collisions *J. High Energy Phys.* JHEP01(2011)152
[32] Eskola K J, Paukkunen H and Salgado C A 2009 EPS09: a new generation of NLO and LO nuclear parton distribution functions *J. High Energy Phys.* JHEP04(2009)065
[33] Kovarik K *et al* 2016 nCTEQ15—global analysis of nuclear parton distributions with uncertainties in the CTEQ framework *Phys. Rev. D* **93** 085037
[34] Garcia O B *et al* 2024 High-density gas target at the LHCb experiment *Phys. Rev. Accel. Beams* **27** 111001
[35] Hadjidakis C *et al* 2021 A fixed-target programme at the LHC: physics case and projected performances for heavy-ion, hadron, spin and astroparticle studies *Phys. Rept.* **911** 1–83
[36] Khalek R A *et al* 2022 Science requirements and detector concepts for the electron-ion collider: EIC yellow report *Nucl. Phys. A* **1026** 122447
[37] Kusina A, Lansberg J-P, Schienbein I and Shao H-S 2018 Gluon shadowing in heavy-flavor production at the LHC *Phys. Rev. Lett.* **121** 052004
[38] Kusina A, Lansberg J-P, Schienbein I and Shao H-S 2021 Reweighted nuclear PDFs using heavy-flavor production data at the LHC *Phys. Rev. D* **104** 014010
[39] Duwentäster P, Ježo T, Klasen M, Kovařík K, Kusina A, Muzakka K F, Olness F I, Ruiz R, Schienbein I and Yu J Y 2022 Impact of heavy quark and quarkonium data on nuclear gluon PDFs *Phys. Rev. D* **105** 114043
[40] Khalek R A, Gauld R, Giani T, Nocera E R, Rabemananjara T R and Rojo J 2022 nNNPDF3.0: evidence for a modified partonic structure in heavy nuclei *Eur. Phys. J. C* **82** 507

[41] Eskola K J, Paakkinen P, Paukkunen H and Salgado C A 2022 EPPS21: a global QCD analysis of nuclear PDFs *Eur. Phys. J. C* **82** 413
[42] Arleo F, Jackson G and Peigné S 2022 Impact of fully coherent energy loss on heavy meson production in pA collisions *J. High Energy Phys.* JHEP01(2022)164
[43] d'Enterria D, Krajczár K and Paukkunen H 2015 Top-quark production in proton-nucleus and nucleus-nucleus collisions at LHC energies and beyond *Phys. Lett. B* **746** 64–72
[44] (CMS Collaboration) 2018 Constraining nuclear parton distributions with heavy ion collisions at the HL-LHC with the CMS experiment *Tech. Rep. CMS-PAS-FTR-18-027* http://cds.cern.ch/record/2652030
[45] Sirunyan A M *et al* (CMS Collaboration) 2017 Observation of top quark production in proton-nucleus collisions *Phys. Rev. Lett.* **119** 242001
[46] Aad G *et al* (ATLAS Collaboration) 2024 Observation of $t\bar{t}$ production in the lepton+jets and dilepton channels in p+Pb collisions at $\sqrt{s_{\mathrm{NN}}} = 8.16$ TeV with the ATLAS detector *J. High Energy Phys.* **11** 101JHEP11(2024)101
[47] (ATLAS Collaboration) 2018 Expected ATLAS measurement capabilities of observables sensitive to nuclear parton distributions *Tech. Rep. ATL-PHYS-PUB-2018-039* https://cds.cern.ch/record/2649445
[48] Stirling W J and Vryonidou E 2012 Charm production in association with an electroweak gauge boson at the LHC *Phys. Rev. Lett.* **109** 082002
[49] Paakkinen P 2022 Light-nuclei gluons from dijet production in proton-oxygen collisions *Phys. Rev. D* **105** L031504
[50] Klein S R and Vogt R 2003 Inhomogeneous shadowing effects on J/ψ production in dA collisions *Phys. Rev. Lett.* **91** 142301
[51] Helenius I, Eskola K J, Honkanen H and Salgado C A 2012 Impact-parameter dependent nuclear parton distribution functions: EPS09s and EKS98s and their applications in nuclear hard processes *J. High Energy Phys.* JHEP07(2012)073
[52] Shao H-S 2020 Probing impact-parameter dependent nuclear parton densities from double parton scatterings in heavy-ion collisions *Phys. Rev. D* **101** 054036
[53] Qiu J-W, Schlegel M and Vogelsang W 2011 Probing gluonic spin–orbit correlations in photon pair production *Phys. Rev. Lett.* **107** 062001
[54] Boer D, den Dunnen W J, Pisano C, Schlegel M and Vogelsang W 2012 Linearly polarized gluons and the Higgs transverse momentum distribution *Phys. Rev. Lett.* **108** 032002
[55] Sun P, Xiao B-W and Yuan F 2011 Gluon distribution functions and Higgs boson production at moderate transverse momentum *Phys. Rev. D* **84** 094005
[56] Boer D, den Dunnen W J, Pisano C and Schlegel M 2013 Determining the Higgs spin and parity in the diphoton decay channel *Phys. Rev. Lett.* **111** 032002
[57] Ma J P, Wang J X and Zhao S 2013 Transverse momentum dependent factorization for quarkonium production at low transverse momentum *Phys. Rev. D* **88** 014027
[58] den Dunnen W J, Lansberg J P, Pisano C and Schlegel M 2014 Accessing the transverse dynamics and polarization of gluons inside the proton at the LHC *Phys. Rev. Lett.* **112** 212001
[59] Lansberg J-P, Pisano C and Schlegel M 2017 Associated production of a dilepton and a $\Upsilon(J/\psi)$ at the LHC as a probe of gluon transverse momentum dependent distributions *Nucl. Phys. B* **920** 192–210
[60] Scarpa F, Boer D, Echevarria M G, Lansberg J-P, Pisano C and Schlegel M 2020 Studies of gluon TMDs and their evolution using quarkonium-pair production at the LHC *Eur. Phys. J. C* **80** 87
[61] Khachatryan V *et al* (CMS Collaboration) 2016 Study of Z boson production in pPb collisions at $\sqrt{s_{NN}} = 5.02$ TeV *Phys. Lett. B* **759** 36–57
[62] Aad G *et al* (ATLAS Collaboration) 2015 Z boson production in p + Pb collisions at $\sqrt{s_{NN}} = 5.02$ TeV measured with the ATLAS detector *Phys. Rev. C* **92** 044915
[63] Alrashed M, Anderle D, Kang Z-B, Terry J and Xing H 2022 Three-dimensional imaging in nuclei *Phys. Rev. Lett.* **129** 242001
[64] Alvioli M, Guzey V and Strikman M 2024 Slicing pomerons in ultraperipheral collisions using forward neutrons from nuclear breakup *Phys. Rev. C* **110** 025205
[65] Pedrak A, Pire B, Szymanowski L and Wagner J 2017 Hard photoproduction of a diphoton with a large invariant mass *Phys. Rev. D* **96** 074008[Erratum: *Phys. Rev. D* **100** 039901]
[66] Grocholski O, Pire B, Sznajder P, Szymanowski L and Wagner J 2021 Collinear factorization of diphoton photoproduction at next to leading order *Phys. Rev. D* **104** 114006

[67] Grocholski O, Pire B, Sznajder P, Szymanowski L and Wagner J 2022 Phenomenology of diphoton photoproduction at next-to-leading order *Phys. Rev. D* **105** 094025
[68] Boussarie R, Pire B, Szymanowski L and Wallon S 2017 Exclusive photoproduction of a $\gamma\,\rho$ pair with a large invariant mass *J. High Energy Phys.* JHEP02(2017)054
Boussarie R, Pire B, Szymanowski L and Wallon S *J. High Energy Phys.* JHEP10(2018)029
[69] Duplančić G, Passek-Kumerički K, Pire B, Szymanowski L and Wallon S 2018 Probing axial quark generalized parton distributions through exclusive photoproduction of a $\gamma\,\pi^{\pm}$ pair with a large invariant mass *J. High Energy Phys.* **2018** 179
[70] Duplančić G, Nabeebaccus S, Passek-Kumerički K, Pire B, Szymanowski L and Wallon S 2023 Accessing chiral-even quark generalised parton distributions in the exclusive photoproduction of a $\gamma\pi^{\pm}$ pair with large invariant mass in both fixed-target and collider experiments *J. High Energy Phys.* **2023** 241
[71] Duplančić G, Nabeebaccus S, Passek-Kumerički K, Pire B, Szymanowski L and Wallon S 2023 Probing chiral-even and chiral-odd leading twist quark generalized parton distributions through the exclusive photoproduction of a $\gamma\rho$ pair *Phys. Rev. D* **107** 094023
[72] El Beiyad M, Pire B, Segond M, Szymanowski L and Wallon S 2010 Photoproduction of a $\pi\rho_T$ pair with a large invariant mass and transversity generalized parton distribution *Phys. Lett. B* **688** 154–67
[73] Chekanov S *et al* (ZEUS Collaboration) 2002 Exclusive photoproduction of J/ψ mesons at HERA *Eur. Phys. J. C* **24** 345–60
[74] Chekanov S *et al* (ZEUS Collaboration) 2004 Exclusive electroproduction of J/ψ mesons at HERA *Nucl. Phys. B* **695** 3–37
[75] Aktas A *et al* (H1 Collaboration) 2006 Elastic J/ψ production at HERA *Eur. Phys. J. C* **46** 585–603
[76] Alexa C *et al* (H1 Collaboration) 2013 Elastic and proton-dissociative photoproduction of J/ψ mesons at HERA *Eur. Phys. J. C* **73** 2466
[77] Aaij R *et al* (LHCb Collaboration) 2018 Central exclusive production of J/ψ and $\psi(2S)$ mesons in pp collisions at $\sqrt{s} = 13$ TeV *J. High Energy Phys.* **2018** 167
[78] Aaij R *et al* (LHCb Collaboration) 2014 Updated measurements of exclusive J/ψ and $\psi(2S)$ production cross-sections in pp collisions at $\sqrt{s} = 7$ TeV *J. Phys. G* **41** 055002
[79] Aaij R *et al* (LHCb Collaboration) 2015 Measurement of the exclusive Υ production cross-section in pp collisions at $\sqrt{s} = 7$ TeV and 8 TeV *J. High Energy Phys.* **2015** 084
[80] Flett C A, Jones S P, Martin A D, Ryskin M G and Teubner T 2022 Exclusive J/ψ and Υ production in high energy pp and pPb collisions *Phys. Rev. D* **106** 074021
[81] Khoze V A, Martin A D and Ryskin M G 2013 Diffraction at the LHC *Eur. Phys. J. C* **73** 2503
[82] Flett C A, Lansberg J P, Nabeebaccus S, Nefedov M, Sznajder P and Wagner J 2024 Exclusive vector-quarkonium photoproduction at NLO in αs in collinear factorisation with evolution of the generalised parton distributions and high-energy resummation *Phys. Lett. B* **859** 139117
[83] Shuvaev A G, Golec-Biernat K J, Martin A D and Ryskin M G 1999 Off diagonal distributions fixed by diagonal partons at small x and ξ *Phys. Rev. D* **60** 014015
[84] Shuvaev A 1999 Solution of the off forward leading logarithmic evolution equation based on the Gegenbauer moments inversion *Phys. Rev. D* **60** 116005
[85] Flett C A, Jones S P, Martin A D, Ryskin M G and Teubner T 2020 How to include exclusive J/ψ production data in global PDF analyses *Phys. Rev. D* **101** 094011
[86] Flett C A, Martin A D, Ryskin M G and Teubner T 2020 Very low x gluon density determined by LHCb exclusive J/ψ data *Phys. Rev. D* **102** 114021
[87] Flett C A, Martin A D, Ryskin M G and Teubner T 2025 A method to include exclusive heavy vector-meson production data at small x in global parton analyses *Eur. Phys. J. C* **85** 434
[88] Flett C 2025 Impact studies of the gluon PDF using exclusive heavy-quarkonium production data *PoS* **ICHEP2024** 585
[89] Flett C A, Jones S P, Martin A D, Ryskin M G and Teubner T 2022 Predictions of exclusive Υ photoproduction at the LHC and future colliders *Phys. Rev. D* **105** 034008
[90] Łuszczak M, Dyndal M, Glazov A and Sadykov R 2019 Probing photonic content of the proton using photon-induced dilepton production in p + Pb collisions at the LHC *Acta Phys. Polon. B* **50** 1117–26
[91] Acharya S *et al* (ALICE Collaboration) 2021 First measurement of the $|t|$-dependence of coherent J/ψ photonuclear production *Phys. Lett. B* **817** 136280

[92] Acharya S *et al* (ALICE Collaboration) 2025 First polarisation measurement of coherently photoproduced J/ψ in ultra-peripheral Pb−Pb collisions at sNN = 5.02 TeV *Phys.Lett.B* **865** 139466
[93] Aad G *et al* (ATLAS Collaboration) 2021 Two-particle azimuthal correlations in photonuclear ultraperipheral Pb+Pb collisions at 5.02 TeV with ATLAS *Phys. Rev. C* **104** 014903
[94] Aad G *et al* (ATLAS Collaboration) 2025 Measurement of photonuclear jet production in ultraperipheral Pb+Pb collisions at $\sqrt{s_{NN}}$ = 5.02 TeV with the ATLAS detector *Phys. Rev. D* **111** 052006
[95] (CMS Collaboration) 2024 *Constraining nuclear parton dynamics with the first measurement of D0-photoproduction in ultraperipheral heavy-ion collisions at the LHC CMS-PAS-HIN-24-003* https://cds.cern.ch/record/2910905
[96] Lansberg J-P, Lynch K, Van Hulse C and McNulty R 2025 Inclusive photoproduction of vector quarkonium in ultra-peripheral collisions at the LHC *Eur.Phys.J.C* **85** 161
[97] Aid S *et al* (H1 Collaboration) 1996 Elastic and inelastic photoproduction of J/ψ mesons at HERA *Nucl. Phys. B* **472** 3–31
[98] Adloff C *et al* (H1 Collaboration) 2002 Inelastic photoproduction of J/ψ mesons at HERA *Eur. Phys. J. C* **25** 25–39
[99] Aaron F D *et al* (H1 Collaboration) 2010 Inelastic production of J/ψ mesons in photoproduction and deep inelastic scattering at HERA *Eur. Phys. J. C* **68** 401–20
[100] Boer D *et al* 2025 Physics case for quarkonium studies at the Electron Ion Collider *Prog. Part. Nucl. Phys.* **142** 104162
[101] Mäntysaari H and Schenke B 2016 Evidence of strong proton shape fluctuations from incoherent diffraction *Phys. Rev. Lett.* **117** 052301
[102] Cepila J, Contreras J G and Tapia Takaki J D 2017 Energy dependence of dissociative J/ψ photoproduction as a signature of gluon saturation at the LHC *Phys. Lett. B* **766** 186–91
[103] (ALICE Collaboration) 2020 Letter of intent: a forward calorimeter (FoCal) in the ALICE experiment *Tech. Rep. CERN-LHCC-2020-009* https://cds.cern.ch/record/2719928
[104] (ALICE Collaboration) 2023 Physics of the ALICE forward calorimeter upgrade *Tech. Rep. ALICE-PUBLIC-2023-001* https://cds.cern.ch/record/2858858
[105] Bylinkin A, Nystrand J and Takaki D T 2023 Vector meson photoproduction in UPCs with FoCal *J. Phys. G* **50** 5
[106] Gribov L, Levin E and Ryskin M 1983 Semihard processes in QCD *Phys. Rept.* **100** 1–150
[107] Mueller A H and Qiu J-w 1986 Gluon recombination and shadowing at small values of *x Nucl. Phys. B* **268** 427–52
[108] Balitsky I 1996 Operator expansion for high-energy scattering *Nucl. Phys. B* **463** 99–160
[109] Kovchegov Y V 1999 Small *x* $F(2)$ structure function of a nucleus including multiple pomeron exchanges *Phys. Rev. D* **60** 034008
[110] Altarelli G and Parisi G 1977 Asymptotic freedom in parton language *Nucl. Phys. B* **126** 298–318
[111] Dokshitzer Y L 1977 Calculation of the structure functions for deep inelastic scattering and e^+ e^- annihilation by perturbation theory in quantum chromodynamics *Sov. Phys. JETP* **46** 641–53
[112] Gelis F, Iancu E, Jalilian-Marian J and Venugopalan R 2010 The color glass condensate *Ann. Rev. Nucl. Part. Sci.* **60** 463–89
[113] Albacete J L and Marquet C 2014 Gluon saturation and initial conditions for relativistic heavy ion collisions *Prog. Part. Nucl. Phys.* **76** 1–42
[114] Blaizot J-P 2017 High gluon densities in heavy ion collisions *Rept. Prog. Phys.* **80** 032301
[115] Arsene I *et al* (BRAHMS Collaboration) 2004 On the evolution of the nuclear modification factors with rapidity and centrality in d + Au collisions at $\sqrt{s_{NN}}$ = 200 GeV *Phys. Rev. Lett.* **93** 242303
[116] Adams J *et al* (STAR Collaboration) 2006 Forward neutral pion production in p+p and d+Au collisions at $\sqrt{s_{NN}}$ = 200 GeV *Phys. Rev. Lett.* **97** 152302
[117] Adare A *et al* (PHENIX Collaboration) 2011 Suppression of back-to-back hadron pairs at forward rapidity in d + Au Collisions at $\sqrt{s_{NN}}$ = 200 GeV *Phys. Rev. Lett.* **107** 172301
[118] Abdallah M S *et al* (STAR Collaboration) 2022 Evidence for nonlinear gluon effects in QCD and their mass number dependence at STAR *Phys. Rev. Lett.* **129** 092501
[119] Chu X and (STAR Collaboration) 2022 Di-π^0 correlations in p+p, p+Al and p+Au collisions at $\sqrt{s_{NN}}$ = 200 GeV at STAR *SciPost Phys. Proc.* **8** 043
[120] Aaij R *et al* (LHCb Collaboration) 2023 Nuclear modification factor of neutral pions in the forward and backward regions in p-Pb collisions *Phys. Rev. Lett.* **131** 042302

[121] Aaij R *et al* (LHCb Collaboration) 2024 Measurement of prompt D^+ and D_s^+ production in pPb collisions at $\sqrt{s_{NN}} = 5.02$ TeV *J. High Energy Phys.* **2024** 070
[122] Mäntysaari H and Tawabutr Y 2024 Complete next-to-leading order calculation of single inclusive π^0 production in forward proton-nucleus collisions *Phys. Rev. D* **109** 034018
[123] Penttala J and Royon C 2025 Gluon saturation effects in exclusive heavy vector meson photoproduction *Phys.Lett.B* **864** 139394
[124] Acharya S *et al* (ALICE Collaboration) 2021 Coherent J/ψ and ψ' photoproduction at midrapidity in ultra-peripheral Pb-Pb collisions at $\sqrt{s_{\rm NN}} = 5.02$ TeV *Eur. Phys. J. C* **81** 712
[125] Acharya S *et al* (ALICE Collaboration) 2023 Energy dependence of coherent photonuclear production of J/ψ mesons in ultra-peripheral Pb-Pb collisions at $\sqrt{s_{\rm NN}} = 5.02$ TeV *J. High Energy Phys.* **2023** 119
[126] Tumasyan A *et al* (CMS Collaboration) 2023 Probing small Bjorken-x nuclear gluonic structure via coherent J/ψ photoproduction in ultraperipheral Pb–Pb collisions at $\sqrt{s_{\rm NN}} = 5.02$ TeV *Phys. Rev. Lett.* **131** 262301
[127] Abelev B B *et al* (ALICE Collaboration) 2014 Exclusive J/ψ photoproduction off protons in ultra-peripheral p-Pb collisions at $\sqrt{s_{\rm NN}} = 5.02$ TeV *Phys. Rev. Lett.* **113** 232504
[128] Acharya S *et al* (ALICE Collaboration) 2019 Energy dependence of exclusive J/ψ photoproduction off protons in ultra-peripheral p-Pb collisions at $\sqrt{s_{\rm NN}} = 5.02$ TeV *Eur. Phys. J. C* **79** 402
[129] Bendova D, Cepila J, Contreras J G and Matas M 2021 Photonuclear J/ψ production at the LHC: proton-based versus nuclear dipole scattering amplitudes *Phys. Lett. B* **817** 136306
[130] Goncalves V P, Moreira B D and Navarra F S 2014 Investigation of diffractive photoproduction of J/Ψ in hadronic collisions *Phys. Rev. C* **90** 015203
[131] Lappi T and Mantysaari H 2013 J/ψ production in ultraperipheral Pb+Pb and p+Pb collisions at energies available at the CERN Large Hadron Collider *Phys. Rev. C* **87** 032201
[132] Aaboud M *et al* (ATLAS Collaboration) 2019 Dijet azimuthal correlations and conditional yields in pp and p+Pb collisions at $\sqrt{s_{\rm NN}} = 5.02$ TeV with the ATLAS detector *Phys. Rev. C* **100** 034903
[133] van Hameren A, Kotko P, Kutak K and Sapeta S 2019 Broadening and saturation effects in dijet azimuthal correlations in p–p and p-Pb collisions at $\sqrt{s} =$ 5.02 TeV *Phys. Lett. B* **795** 511–5
[134] Sirunyan A M *et al* (CMS Collaboration) 2019 Measurement of inclusive very forward jet cross sections in proton-lead collisions at $\sqrt{s_{\rm NN}} = 5.02$ TeV *J. High Energy Phys.* **2019** 043
[135] Bury M, Van Haevermaet H, Van Hameren A, Van Mechelen P, Kutak K and Serino M 2018 Single inclusive jet production and the nuclear modification ratio at very forward rapidity in proton-lead collisions with $\sqrt{s_{NN}} = 5.02$ TeV *Phys. Lett. B* **780** 185–90
[136] Mäntysaari H and Paukkunen H 2019 Saturation and forward jets in proton-lead collisions at the LHC *Phys. Rev. D* **100** 114029
[137] Liu H-y, Xie K, Kang Z and Liu X 2022 Single inclusive jet production in pA collisions at NLO in the small-x regime *J. High Energy Phys.* JHEP07(2022)041
[138] Dominguez F, Marquet C, Xiao B-W and Yuan F 2011 Universality of unintegrated gluon distributions at small x *Phys. Rev. D* **83** 105005
[139] Jalilian-Marian J and Rezaeian A H 2012 Prompt photon production and photon-hadron correlations at RHIC and the LHC from the color glass condensate *Phys. Rev. D* **86** 034016
[140] Rezaeian A H 2012 Semi-inclusive photon-hadron production in pp and pA collisions at RHIC and LHC *Phys. Rev. D* **86** 094016
[141] Benić S, Garcia-Montero O and Perkov A 2022 Isolated photon-hadron production in high energy pp and pA collisions at RHIC and LHC *Phys. Rev. D* **105** 114052
[142] Ganguli I, van Hameren A, Kotko P and Kutak K 2023 Forward γ+jet production in proton-proton and proton-lead collisions at LHC within the FoCal calorimeter acceptance *Eur. Phys. J. C* **83** 868
[143] Boussarie R *et al* 2023 TMD handbook JLAB-THY-23-3780 arXiv:2304.03302
[144] Collins J 2011 *Foundations of Perturbative QCD* vol 32 (Cambridge University Press) (https://doi.org/10.1017/CBO9780511975592)
[145] Kotko P, Kutak K, Sapeta S, Stasto A M and Strikman M 2017 Estimating nonlinear effects in forward dijet production in ultra-peripheral heavy ion collisions at the LHC *Eur. Phys. J. C* **77** 353
[146] Boussarie R, Grabovsky A V, Szymanowski L and Wallon S 2014 Impact factor for high-energy two and three jets diffractive production *J. High Energy Phys.* JHEP09(2014)026

[147] Boussarie R, Grabovsky A V, Szymanowski L and Wallon S 2016 On the one loop $\gamma^{(*)} \to q\bar{q}$ impact factor and the exclusive diffractive cross sections for the production of two or three jets *J. High Energy Phys.* JHEP11(2016)149
[148] Iancu E, Mueller A H and Triantafyllopoulos D N 2022 Probing parton saturation and the gluon dipole via diffractive jet production at the electron-ion collider *Phys. Rev. Lett.* **128** 202001
[149] Jalilian-Marian J and Rezaeian A H 2012 Hadron production in *pA* collisions at the LHC from the color glass condensate *Phys. Rev. D* **85** 014017
[150] van Hameren A, Kakkad H, Kotko P, Kutak K and Sapeta S 2023 Searching for saturation in forward dijet production at the LHC *Eur. Phys. J. C* **83** 947
[151] Kang Z-B, Lee S, Penttala J, Zhao F and Zhou Y 2025 Transverse energy-energy correlator for vector boson-tagged hadron production in *pp* and *pA* collisions *Phys. Rev. D* **112** 014012
[152] Enberg R, Forshaw J R, Motyka L and Poludniowski G 2003 Vector meson photoproduction from the BFKL equation: I. theory *J. High Energy Phys.* JHEP09(2003)008
[153] Poludniowski G G, Enberg R, Forshaw J R and Motyka L 2003 Vector meson photoproduction from the BFKL equation: II. phenomenology *J. High Energy Phys.* JHEP12(2003)002
[154] Boussarie R, Grabovsky A V, Ivanov D Y, Szymanowski L and Wallon S 2017 Next-to-leading order computation of exclusive diffractive light vector meson production in a saturation framework *Phys. Rev. Lett.* **119** 072002
[155] Boussarie R, Fucilla M, Szymanowski L and Wallon S 2025 Twist corrections to exclusive vector meson production in a saturation framework *Phys. Rev. D* **111** 014032
[156] Boussarie R, Fucilla M, Szymanowski L and Wallon S 2025 Probing gluonic saturation in deeply virtual meson production beyond leading power *Phys. Rev. Lett.* **134** 041901
[157] Fucilla M, Grabovsky A, Li E, Szymanowski L and Wallon S 2024 Diffractive single hadron production in a saturation framework at the NLO *J. High Energy Phys.* JHEP02(2024)165
[158] Fucilla M, Grabovsky A V, Li E, Szymanowski L and Wallon S 2023 NLO computation of diffractive di-hadron production in a saturation framework *J. High Energy Phys.* JHEP03(2023)159
[159] Abazov V M *et al* (D0, TOTEM Collaboration) 2021 Odderon exchange from elastic scattering differences between *pp* and $p\bar{p}$ data at 1.96 TeV and from pp forward scattering measurements *Phys. Rev. Lett.* **127** 062003
[160] Hagler P, Pire B, Szymanowski L and Teryaev O V 2002 Pomeron–odderon interference effects in electroproduction of two pions *Eur. Phys. J. C* **26** 261–70
[161] McNulty R, Khoze V A, Martin A D and Ryskin M G 2020 Isolating the Odderon in central production in high energy *pA* and *AA* collisions *Eur. Phys. J. C* **80** 288
[162] Bzdak A, Motyka L, Szymanowski L and Cudell J R 2007 Exclusive J/ψ and Υ hadroproduction and the QCD odderon *Phys. Rev. D* **75** 094023
[163] Accardi A, Arleo F, Brooks W K, D'Enterria D and Muccifora V 2009 Parton propagation and fragmentation in QCD matter *Riv. Nuovo Cim.* **32** 439–554
[164] Khachatryan V *et al* (CMS Collaboration) 2010 Observation of long-range near-side angular correlations in proton-proton collisions at the LHC *J. High Energy Phys.* **2010** 091
[165] Abelev B *et al* (ALICE Collaboration) 2013 Long-range angular correlations on the near and away side in *p*-Pb collisions at $\sqrt{s_{NN}} = 5.02$ TeV *Phys. Lett. B* **719** 29–41
[166] Aad G *et al* (ATLAS Collaboration) 2013 Observation of associated near-side and away-side long-range correlations in $\sqrt{s_{NN}} = 5.02$ TeV proton-lead collisions with the ATLAS detector *Phys. Rev. Lett.* **110** 182302
[167] Khachatryan V *et al* (CMS Collaboration) 2015 Evidence for collective multiparticle correlations in *p*-Pb collisions *Phys. Rev. Lett.* **115** 012301
[168] Noronha J, Schenke B, Shen C and Zhao W 2024 Progress and challenges in small systems *Int. J. Mod. Phys. E* **33** 2430005
[169] Lisa M A, Barbon J a G P, Chinellato D D, Serenone W M, Shen C, Takahashi J and Torrieri G 2021 Vortex rings from high energy central *p*+*A* collisions *Phys. Rev. C* **104** 011901
[170] Dobrigkeit Chinellato D, Lisa M A, Matioli Serenone W, Shen C, Takahashi J and Torrieri G 2024 Vortex rings in event-by-event relativistic heavy-ion collisions *Phys. Rev. C* **110** 054908
[171] Diehl M, Ostermeier D and Schafer A 2012 Elements of a theory for multiparton interactions in QCD *J. High Energy Phys.* JHEP03(2012)089
Diehl M, Ostermeier D and Schafer A 2016 JHEP03(2016)001
[172] Gaunt J R and Stirling W J 2010 Double parton distributions incorporating perturbative QCD evolution and momentum and quark number sum rules *J. High Energy Phys.* JHEP03(2010)005

[173] d'Enterria D and Snigirev A M 2017 Triple parton scatterings in high-energy proton-proton collisions *Phys. Rev. Lett.* **118** 122001
[174] Rinaldi M and Ceccopieri F A 2018 Hadronic structure from double parton scattering *Phys. Rev. D* **97** 071501
[175] Tumasyan A *et al* (CMS Collaboration) 2023 Observation of same-sign WW production from double parton scattering in proton-proton collisions at $\sqrt{s} = 13$ TeV *Phys. Rev. Lett.* **131** 091803
[176] d'Enterria D and Snigirev A 2018 Double, triple, and *n*-parton scatterings in high-energy proton and nuclear collisions *Adv. Ser. Direct. High Energy Phys.* **29** 159–87
[177] Strikman M and Treleani D 2002 Measuring double parton distributions in nucleons at proton nucleus colliders *Phys. Rev. Lett.* **88** 031801
[178] Cattaruzza E, Del Fabbro A and Treleani D 2004 Heavy-quark production in proton-nucleus collision at the CERN LHC *Phys. Rev. D* **70** 034022
[179] d'Enterria D and Snigirev A M 2013 Same-sign WW production in proton-nucleus collisions at the LHC as a signal for double parton scattering *Phys. Lett. B* **718** 1395–400
[180] Blok B, Strikman M and Wiedemann U A 2013 Hard four-jet production in *pA* collisions *Eur. Phys. J. C* **73** 2433
[181] d'Enterria D and Snigirev A M 2014 Pair production of quarkonia and electroweak bosons from double-parton scatterings in nuclear collisions at the LHC *Nucl. Phys. A* **931** 303–8
[182] d'Enterria D and Snigirev A M 2013 Enhanced J/Ψ-pair production from double parton scatterings in nucleus-nucleus collisions at the Large Hadron Collider *Phys. Lett. B* **727** 157–62
[183] Blok B and Strikman M 2018 Multiparton *pp* and *pA* collisions: from geometry to parton–parton correlations *Adv. Ser. Direct. High Energy Phys.* **29** 63–99
[184] Tumasyan A *et al* (CMS Collaboration) 2023 Observation of triple J/ψ meson production in proton-proton collisions *Nature Phys* **19** 338–50[Erratum: *Nature Phys. D* **19** 461]
[185] Lansberg J-P 2020 New observables in inclusive production of quarkonia *Phys. Rept.* **889** 1–106
[186] Lansberg J-P, Shao H-S and Yamanaka N 2018 Indication for double parton scatterings in $W +$ prompt J/ψ production at the LHC *Phys. Lett. B* **781** 485–91
[187] Lansberg J-P and Shao H-S 2016 Associated production of a quarkonium and a *Z* boson at one loop in a quark-hadron-duality approach *J. High Energy Phys.* JHEP10(2016)153
[188] Aaboud M *et al* (ATLAS Collaboration) 2017 Measurement of the prompt J/ ψ pair production cross-section in pp collisions at $\sqrt{s} = 8$ TeV with the ATLAS detector *Eur. Phys. J. C* **77** 76
[189] Lansberg J-P and Shao H-S 2015 J/ψ -pair production at large momenta: indications for double parton scatterings and large α_s^5 contributions *Phys. Lett. B* **751** 479–86
[190] Hayrapetyan *et al* (CMS Collaboration) 2024 Observation of double J/ψ meson production in *p*Pb collisions at $\sqrt{s_{NN}} = 8.16$ TeV *Phys. Rev. D* **110** 092002
[191] d'Enterria D and Snigirev A M 2018 Charm, bottom, and quarkonia cross sections for double and triple-parton scatterings in high-energy proton-nucleus and nucleus-nucleus collisions *PoS HardProbes 2018* p 132
[192] Aaij R *et al* (LHCb Collaboration) 2020 Observation of enhanced double parton scattering in proton-lead collisions at $\sqrt{s_{NN}} = 8.16$ TeV *Phys. Rev. Lett.* **125** 212001
[193] Cotogno S, Kasemets T and Myska M 2020 Confronting same-sign *W*-boson production with parton correlations *J. High Energy Phys.* JHEP10(2020)214
[194] Ceccopieri F A, Rinaldi M and Scopetta S 2017 Parton correlations in same-sign *W* pair production via double parton scattering at the LHC *Phys. Rev. D* **95** 114030
[195] Alvioli M, Azarkin M, Blok B and Strikman M 2019 Revealing minijet dynamics via centrality dependence of double parton interactions in proton-nucleus collisions *Eur. Phys. J. C* **79** 482
[196] d'Enterria D and Snigirev A M 2018 Triple-parton scatterings in proton-nucleus collisions at high energies *Eur. Phys. J. C* **78** 359
[197] Maneyro M and d'Enterria D 2025 Six-jet production from triple parton scatterings in proton-proton collisions at the LHC *PoS* **DIS2024** 189
[198] Aaij R *et al* (LHCb Collaboration) 2024 Fraction of χc decays in prompt J/ψ production measured in pPb collisions at $\sqrt{s_{NN}} = 8.16$ TeV *Phys. Rev. Lett.* **132** 102302
[199] Aaij R *et al* (LHCb Collaboration) 2018 Study of Υ production in *p*Pb collisions at $\sqrt{s_{NN}} = 8.16$ TeV *J. High Energy Phys.* **2018** 194 [Erratum: 2020JHEP02(2020)093]
[200] Aaij R *et al* (LHCb Collaboration) 2014 Study of χ_b meson production in pp collisions at $\sqrt{s} = 7$ and 8 TeV and observation of the decay $\chi_b(3P) \to \Upsilon(3S)\gamma$ *Eur. Phys. J. C* **74** 3092

[201] (LHCb Collaboration) 2021 List of hadrons observed at the LHC, LHCB-FIGURE-2021-001, https://cds.cern.ch/record/2749030 See update online at https://www.koppenburg.ch/particles.html
[202] Aaij R *et al* (LHCb Collaboration) 2024 Modification of χc1(3872) and ψ(2S) production in pPb collisions at $\sqrt{s_{\rm NN}} = 8.16$ TeV *Phys. Rev. Lett.* **132** 242301
[203] Cho S *et al* (ExHIC Collaboration) 2017 Exotic hadrons from heavy ion collisions *Prog. Part. Nucl. Phys.* **95** 279–322
[204] Esposito A, Ferreiro E G, Pilloni A, Polosa A D and Salgado C A 2021 The nature of *X*(3872) from high-multiplicity pp collisions *Eur. Phys. J. C* **81** 669
[205] Vogt R 2024 Tetraquarks from intrinsic heavy quarks *Phys. Rev. D* **110** 074036
[206] d'Enterria D and Lansberg J-P 2010 Study of Higgs boson production and its $b\bar{b}$ decay in $\gamma\gamma$ processes in proton-nucleus collisions at the LHC *Phys. Rev. D* **81** 014004
[207] Aad G *et al* (ATLAS Collaboration) 2021 Exclusive dimuon production in ultraperipheral Pb +Pb collisions at $\sqrt{s_{\rm NN}} = 5.02$ TeV with ATLAS *Phys. Rev. C* **104** 024906
[208] Aad G *et al* (ATLAS Collaboration) 2023 Exclusive dielectron production in ultraperipheral Pb +Pb collisions at $\sqrt{s_{\rm NN}} = 5.02$ TeV with ATLAS *J. High Energy Phys.* **2023** 182
[209] Aad G *et al* (ATLAS Collaboration) 2020 Observation and measurement of forward proton scattering in association with lepton pairs produced via the photon fusion mechanism at ATLAS *Phys. Rev. Lett.* **125** 261801
[210] Harland-Lang L A, Tasevsky M, Khoze V A and Ryskin M G 2020 A new approach to modelling elastic and inelastic photon-initiated production at the LHC: SuperChic 4 *Eur. Phys. J. C* **80** 925
[211] Shao H-S and d'Enterria D 2025 Dimuon and ditau production in photon–photon collisions at next-to-leading order in QED *J. High Energy Phys.* JHEP02(2025)023
[212] Dreyer U, Hencken K and Trautmann D 2009 Testing the electroweak gauge boson coupling in exclusive photoproduction of single W bosons at the LHC *J. Phys. G* **36** 085003
[213] Abelev B *et al* (ALICE Collaboration) 2012 Measurement of the cross section for electromagnetic dissociation with neutron emission in Pb–Pb collisions at $\sqrt{s_{NN}} = 2.76$ TeV *Phys. Rev. Lett.* **109** 252302
[214] Sirunyan A M *et al* (CMS Collaboration) 2021 Observation of forward neutron multiplicity dependence of dimuon acoplanarity in ultraperipheral Pb–Pb collisions at $\sqrt{s_{NN}} = 5.02$ TeV *Phys. Rev. Lett.* **127** 122001
[215] Acharya S *et al* (ALICE Collaboration) 2023 Neutron emission in ultraperipheral Pb-Pb collisions at $\sqrt{s_{NN}} = 5.02$ TeV *Phys. Rev. C* **107** 064902
[216] Hayrapetyan A *et al* (CMS Collaboration) 2024 Measurement of light-by-light scattering and the Breit-Wheeler process, and search for axion-like particles in ultraperipheral PbPb collisions at $\sqrt{s_{\rm NN}} = 5.02$ TeV arXiv:2412.15413
[217] Aad G *et al* (ATLAS Collaboration) 2025 Search for magnetic monopole pair production in ultraperipheral Pb+Pb collisions at $\sqrt{s_{\rm NN}} = 5.36$ TeV with the ATLAS detector at the LHC *Phys. Rev. Lett.* **134** 061803
[218] Bruce R *et al* 2020 New physics searches with heavy-ion collisions at the CERN Large Hadron Collider *J. Phys. G* **47** 060501
[219] d'Enterria D *et al* 2023 Opportunities for new physics searches with heavy ions at colliders *J. Phys. G* **50** 050501
[220] Knapen S, Lin T, Lou H K and Melia T 2017 Searching for axionlike particles with ultraperipheral heavy-ion collisions *Phys. Rev. Lett.* **118** 171801
[221] Fichet S, von Gersdorff G, Lenzi B, Royon C and Saimpert M 2015 Light-by-light scattering with intact protons at the LHC: from standard model to new physics *J. High Energy Phys.* JHEP02(2015)165
[222] Fichet S and von Gersdorff G 2015 Effective theory for neutral resonances and a statistical dissection of the ATLAS diboson excess *J. High Energy Phys.* JHEP12(2015)089
[223] Baldenegro C, Bellora A, Fichet S, von Gersdorff G, Pitt M and Royon C 2022 Searching for anomalous top quark interactions with proton tagging and timing detectors at the LHC *J. High Energy Phys.* JHEP08(2022)021
[224] Fichet S and von Gersdorff G 2014 Anomalous gauge couplings from composite Higgs and warped extra dimensions *J. High Energy Phys.* JHEP03(2014)102
[225] Megìas E and Quirós M 2019 Gapped continuum Kaluza-Klein spectrum *J. High Energy Phys.* JHEP08(2019)166

[226] Fichet S, Megias E and Quiros M 2023 Continuum effective field theories, gravity, and holography *Phys. Rev. D* **107** 096016
[227] Peccei R D and Quinn H R 1977 CP conservation in the presence of instantons *Phys. Rev. Lett.* **38** 1440–3
[228] Peccei R D and Quinn H R 1977 CP conservation in the presence of pseudoparticles *Phys. Rev. Lett.* **38** 1440–3
[229] Witten E 1984 Some properties of O(32) superstrings *Phys. Lett. B* **149** 351–6
[230] Conlon J P 2006 The QCD axion and moduli stabilisation *J. High Energy Phys.* JHEP05(2006)078
[231] Svrcek P and Witten E 2006 Axions in string theory *J. High Energy Phys.* JHEP06(2006)051
[232] Arvanitaki A, Dimopoulos S, Dubovsky S, Kaloper N and March-Russell J 2010 String axiverse *Phys. Rev. D* **81** 123530
[233] Acharya B S, Bobkov K and Kumar P 2010 An M theory solution to the strong CP problem and constraints on the axiverse *J. High Energy Phys.* JHEP11(2010)105
[234] Cicoli M, Goodsell M and Ringwald A 2012 The type IIB string axiverse and its low-energy phenomenology *J. High Energy Phys.* JHEP10(2012)146
[235] Massó E and Toldrà R 1995 On a light spinless particle coupled to photons *Phys. Rev. D* **52** 1755–63
[236] Csaki C, Graesser M L and Kribs G D 2001 Radion dynamics and electroweak physics *Phys. Rev. D* **63** 065002
[237] Goldberger W D, Grinstein B and Skiba W 2008 Distinguishing the Higgs boson from the dilaton at the Large Hadron Collider *Phys. Rev. Lett.* **100** 111802
[238] Fichet S, von Gersdorff G, Pontón E and Rosenfeld R 2016 The excitation of the global symmetry-breaking vacuum in composite Higgs models *J. High Energy Phys.* JHEP09(2016)158
[239] Fichet S 2017 Shining light on polarizable dark particles *J. High Energy Phys.* JHEP04(2017)088
[240] Gunion J F, Haber H E, Kane G L and Dawson S 2000 *The Higgs Hunter's Guide* Frontiers in Physics Book 80 (CRC Press) (https://doi.org/10.1201/9780429496448)
[241] Englert C, Plehn T, Zerwas D and Zerwas P M 2011 Exploring the Higgs portal *Phys. Lett. B* **703** 298–305
[242] Csaki C 2004 TASI lectures on extra dimensions and branes arXiv:hep-ph/0404096
[243] Baldenegro C, Fichet S, von Gersdorff G and Royon C 2017 Probing the anomalous $\gamma\gamma$Z coupling at the LHC with proton tagging *J. High Energy Phys.* JHEP06(2017)142
[244] Gibbons G W 1998 Born-infeld particles and Dirichlet p-branes *Nucl. Phys. B* **514** 603–39
[245] Davila J M, Schubert C and Trejo M A 2014 Photonic processes in Born-infeld theory *Int. J. Mod. Phys. A* **29** 1450174
[246] Ellis J, Mavromatos N E and You T 2017 Light-by-light scattering constraint on born-infeld theory *Phys. Rev. Lett.* **118** 261802
[247] Randall L and Sundrum R 1999 An alternative to compactification *Phys. Rev. Lett.* **83** 4690–3
[248] Strassler M J 2003 Why unparticle models with mass gaps are examples of hidden valleys arXiv:0801.0629
[249] Friedland A, Giannotti M and Graesser M 2009 On the RS2 realization of unparticles *Phys. Lett. B* **678** 149–55
[250] Friedland A, Giannotti M and Graesser M L 2009 Vector Bosons in the Randall-Sundrum 2 and Lykken-Randall models and unparticles *J. High Energy Phys.* JHEP09(2009)033
[251] Chaffey I, Fichet S and Tanedo P 2024 Holography of broken $U(1)$ symmetry *J. High Energy Phys.* JHEP05(2024)330
[252] Megias E and Quiros M 2021 Analytical green's functions for continuum spectra *J. High Energy Phys.* JHEP09(2021)157
[253] Fichet S, Megias E and Quiros M 2024 Holography of linear dilaton spacetimes from the bottom up *Phys. Rev. D* **109** 106011
[254] Fichet S, Megias E and Quiros M 2024 Holographic fluids from 5D dilaton gravity *J. High Energy Phys.* JHEP08(2024)077
[255] McDonald K L and Morrissey D E 2010 Low-energy probes of a warped extra dimension *J. High Energy Phys.* JHEP05(2010)056
[256] von Harling B and McDonald K L 2012 Secluded dark matter coupled to a hidden CFT *J. High Energy Phys.* JHEP08(2012)048
[257] Brax P, Fichet S and Tanedo P 2019 The warped dark sector *Phys. Lett. B* **798** 135012

[258] Kampert K-H and Unger M 2012 Measurements of the cosmic ray composition with air shower experiments *Astropart. Phys.* **35** 660–78
[259] Aab A *et al* (Pierre Auger Collaboration) 2020 Direct measurement of the muonic content of extensive air showers between 2×10^{17} and 2×10^{18} eV at the Pierre Auger observatory *Eur. Phys. J. C* **80** 751
[260] Aab A *et al* (Pierre Auger Collaboration) 2021 Measurement of the fluctuations in the number of muons in extensive air showers with the Pierre Auger observatory *Phys. Rev. Lett.* **126** 152002
[261] Cazon L 2020 Working group report on the combined analysis of muon density measurements from eight air shower experiments (EAS-MSU, IceCube, KASCADE Grande, NEVOD-DECOR, Pierre Auger, SUGAR, Telescope Array, and Yakutsk EAS Array collaborations) *PoS* **ICRC2019** 214
[262] Abdul Halim A *et al* (Pierre Auger Collaboration) 2024 Testing hadronic-model predictions of depth of maximum of air-shower profiles and ground-particle signals using hybrid data of the Pierre Auger observatory *Phys. Rev. D* **109** 102001
[263] Albrecht J *et al* 2022 The Muon Puzzle in cosmic-ray induced air showers and its connection to the Large Hadron Collider *Astrophys. Space Sci.* **367** 27
[264] Pierog T and Werner K 2023 EPOS LHC-R: up-to-date hadronic model for EAS simulations *PoS* **ICRC2023** 230
[265] Aartsen M G *et al* (IceCube Collaboration) 2013 Evidence for high-energy extraterrestrial neutrinos at the icecube detector *Science* **342** 1242856
[266] Aartsen M G *et al* (IceCube Collaboration) 2014 Observation of high-energy astrophysical neutrinos in three years of icecube data *Phys. Rev. Lett.* **113** 101101
[267] Goncalves V P, Maciuła R, Pasechnik R and Szczurek A 2017 Mapping the dominant regions of the phase space associated with $c\bar{c}$ production relevant for the prompt atmospheric neutrino flux *Phys. Rev. D* **96** 094026
[268] Azzi P *et al* 2019 Report from working group 1: standard model physics at the HL-LHC and HE-LHC *CERN Yellow Rep. Monogr.* **7** 1–220